

**Age-specific changes of mesenchymal stem cells are paralleled by
upregulation of CD106 expression as a response to an
inflammatory environment**

Gerhard T. Laschober^{1,*}, Regina Brunauer^{1,*}, Angelika Jamnig¹, Sarvpreet Singh¹,
Ulrich Hafen¹, Christine Fehrer¹, Frank Kloss², Robert Gassner², Günter
Lepperdinger¹

¹ Extracellular Matrix Research, Institute for Biomedical Aging Research, Austrian
Academy of Sciences, Rennweg 10, A-6020 Innsbruck

² Department for Cranio-, Maxillofacial & Oral Surgery, University Hospital Innsbruck,
Maximilian Str. 10, A-6020 Innsbruck

* contributed equally

address for correspondence and reprints: Dr. Günter Lepperdinger, Institute for
Biomedical Aging Research, Austrian Academy of Sciences, Rennweg 10, A-6020
Innsbruck; t: 0043 512 5839 1940, f: 0043 512 5839 198, e:
Guenther.Lepperdinger@oeaw.ac.at

Word count: 4410 (main text - excluding abstract, figures, legend, and references)

Short title: Age-Related Changes in Mesenchymal Stem Cells

Keywords: mesenchymal stem cells, aging, inflammation, differentiation,
commitment, regeneration

Abstract

Regeneration, tissue remodeling and organ repair after injury which rely on the regulated activity of tissue-borne stem cells become increasingly compromised with advancing age.

Mesenchymal stroma cells were isolated from bone of differently aged healthy donors. The rare population of mesenchymal stem cells (MSC) contained in the primary cell isolates, barely declined in number, yet relative to the donor age the stem cells displayed diminished long-term proliferation potential. The expression of vascular cell adhesion molecule 1 (CD106) was elevated on primary MSC. In CD106^{bright} MSC, the abundance of a panel of stemness transcription factors remained unchanged. As the CD106 level could be further enhanced by pro-inflammatory cytokines, we considered the rate of VCAM1 expression a good reflection of an endogenous inflammatory milieu MSC are exposed to. Treatment of MSC with increasing doses of interferon gamma exerted no immediate influence on their self-renewal capacity. It however impacted on the differentiation potential towards the adipogenic or osteogenic lineage. Moderately elevated levels of inflammatory stimuli supported osteoblastogenesis while the same treatment reduced adipogenic differentiation in MSC from young and intermediately aged donors. In mesenchymal stem cells from elderly donors however, osteoblastogenesis was greatly diminished in an inflammatory environment whereas adipogenic differentiation remained unchanged.

Conclusively, moderate levels of inflammatory stimuli are being interpreted by mesenchymal stem cells at young age as instructive signals for osteoblastogenesis, whereas at old age, an inflammatory milieu may effectively suppress bone remodeling and repair by tissue-borne mesenchymal stem cells while uninterrupted adipogenic differentiation may lead to adipose upgrowth.

Introduction

Mesenchymal stem cells (1), also called mesenchymal stromal cells (MSC) (2) are present in many adult tissues and are thus considered attractive assets for regenerative medicine (3,4). MSC have been defined as undifferentiated cells, being able to self-renew with a high proliferative capacity, and capable of forming different types of progeny (5). Mesenchymal progenitors also appear to be important determinants in the regulation of hematopoiesis, as these cells give rise to hematopoietic supportive stroma (6).

Much work in adult stem cell biology and regenerative medicine has focused on isolated MSC in culture. Presently, MSC are being isolated and cultured following different methods and protocols. It is therefore difficult to resolve how results regarding ex vivo propagated cells relate to each other. A large body of information is available on many aspects of cultivated MSC properties, while there is still little consensus on their ex vivo antigenic definition. Early on, CD105 and CD73 have been reported indispensable markers (1), furthermore CD29, CD44, and CD90 are pertinent determinants (7). STRO-1 antibody (recognizing CD146) identifies an immature population of mesenchymal cells (8), and many other factors have been studied as well (for further reading please see (9)). Interestingly, Prockop and coworkers discovered that one particular type of MSC, RS cells, cannot be clearly distinguished from other adherent mesenchymal cells solely by surface marker expression (2,10).

Since there is no universal antigenic definition of MSC, analogous to CD34 for hematopoietic stem cells, and there is no universal assay, analogous to hematopoietic repopulation assays, there is only little data available from *in vivo* experimentation comparing the ability of MSC obtained from different tissues, in particular with respect to their differentiation potential and proliferation capacity (11).

As primary MSC are being isolated from individuals of different age and life history, an important question concerns their overall fitness in general, as well as any manifestations resulting from age-related insults, which are in due course affecting basic stem cell properties (12-14). As organisms are facing perpetual attacks by extrinsic agents and harmful sources, pro-inflammatory signals which in concert with other defense mechanisms exert a beneficial role earlier in life, act in an antagonistic way later in life. Consequently chronic exposure to a variety of antigens, can induce a chronic low-grade inflammatory status that may also impact on naïve stem cells residing in their niches, and deviation thereof may thus contribute to age-associated morbidity and mortality (15).

Hence to date, no objective clinical recommendations regarding the optimal MSC population for distinct therapies can be given either (16).

This in mind, two fundamental questions in stem cell biogerontology need to be addressed: *(i)* are MSC subject to intrinsic or extrinsic aging, and in this respect, which type of age-associated changes do recur in primary MSC isolates, in particular regarding their proliferation capacity and differentiation potential; *(ii)* is it possible to single out valid markers to select and ultimately gear the most appropriate MSC subpopulation into biomedical applications, e.g. in tissue engineering or immune modulation therapy?

Material and Methods

MSC explanation, culture and in vitro differentiation

MSC were isolated from the iliac crest of systemically healthy individuals which had been harvested for reconstructive bone surgery of defects within other areas of the body. A small biopsy of *substantia spongiosa osseum*, which otherwise would have been discarded based on necessary bone for molding and recontouring prior to insertion into the recipient site was taken to further investigation under an Institutional Review Board-approved protocol after having obtained patients' written consent (in case of children written consent was given by parents or the respective legal guardian). Isolation, culture and differentiation in vitro were performed as described previously (17). Briefly, MSC were cultivated (MEM supplemented with 20% fetal calf serum, 100 units/mL penicillin, 100 µg/mL streptomycin,) at ambient atmosphere, 5% CO₂, 37°C (Heracell) as well as at 3% O₂, 5% CO₂, 37°C (Thermo Electron Corporation 3110). Before reaching confluency, cells were trypsinized and re-seeded at a density of 50 cells / cm² in order to select for MSC which exhibited clonogenic growth. For differentiation, MSC were plated at 50 cells/cm², grown to near confluence and then induced to differentiate. The induction medium was changed twice per week for a period of three weeks. Osteogenesis was stimulated using growth medium containing 1 mM β-glycerol phosphate, 100 nM dexamethasone, and 0.5 µM ascorbate-2-phosphate. For evaluation, the cells were fixed with 4% *para*-formaldehyde / PBS for 10 minutes and stained with Alizarin Red, pH 4.1 and in parallel lysed and processed for qRT-PCR analysis. For adipogenic differentiation of MSC, growth medium was supplemented with 1 µM dexamethasone, 60 µM indomethacine, 0.5 mM 3-*iso*-butyl-1-methylxanthine, and 0.5 µM hydrocortisone. After fixation, lipid vesicles in differentiated cells were stained

with 0.7% Oil Red O in 85% propylene glycol and in parallel lysed and processed for qRT-PCR analysis.

Treatment with varying doses of human recombinant interferon gamma (Peprotech) up to 100 U/ml, the latter corresponding to 5 pg/ml was carried out for 24h.. For long-term culture, cells were thawed, cultured in the presence of 10 U/ml IFN γ from day 7 on, and passaged as described before until replicative senescence. For differentiation in presence of IFN γ , cells were grown to 70% confluence, treated with various IFN γ concentrations for 3 days, differentiated as described before in presence of the respective amount of IFN γ , and analysed by histological stainings and qPCR.

RNA Isolation, Genomic Analysis, Quantitative Reverse Transcription-Polymerase Chain Reaction

RNA was isolated from cells after homogenization in 4.2 M guanidinium thiocyanate, phenol extraction and ethanol precipitation. Total mRNA was further processed for micro array analysis according to Affymetrix standardized procedures prior to hybridization onto Affymetrix Human Genome HG-133 Plus 2.0 arrays. Raw data were jointly normalized using CARMAweb (18) by means of the gcrma algorithm. For reverse-transcription PCR analysis, cDNA was synthesized from total RNA using RevertAid H Minus-MMuLV-RT (Fermentas, St. Leon-Roth, Germany) and oligo(dT) primer (MWG, Germany). The assays were performed on a LightCycler 480 instrument (Roche, Austria) with the LC480-SYBR Green I Master kit (Roche, Austria). The 16 μ L reactions contained 0.9 μ M forward and reverse primer. After the activation of the enzyme at 95°C for 8 minutes, 50 cycles at 95°C for 15 seconds, 57°C for 8 seconds and 72°C for 15 seconds were performed. mRNA expression levels were calculated relative to eukaryotic translation elongation factor 1 alpha 1

(EEF1A1) using the $\Delta\Delta C_t$ method. Primer sequences and transcript IDs of the corresponding genes were as summarized as in Supplementary Table 4. Primer efficiency and detection ranges were tested for each primer pair employing standard curves.

Antibody staining for Flow Cytometry / Fluorescence-Activated Cell Sorting and Microscopy

Cells were harvested by first adding 0.05% trypsin-EDTA, next washing and suspending them in PBS. 50 μ L aliquots ($0.2 - 1 \times 10^6$ cells) were incubated with 20 μ L PE-conjugated CD106 antibody (BD Pharmingen, #555647) or isotype control (BD Pharmingen, #555792) in the dark at 4°C for 30 minutes and washed with PBS. CD106 protein expression was analyzed with the aid of a FACSCanto[®] flow cytometer and FACSDiva[®] Software (BD Pharmingen). Dead cells were stained with Annexin V FITC and 7-aminoactinomycin (7-AAD).

For fluorescence-activated cell sorting, cells were stained against CD106 as described above. Dead cells were stained with Annexin V FITC (BD Pharmingen, #556420) according to the manufacturer's protocol. Samples were resuspended in PBS supplemented with 2 mM EDTA and passed through a 100 μ m nylon sieve. With the aid of a FACSVantage SE[®] cell sorter (BD Pharmingen), living cells were separated into fractions containing CD106 bright and dim subpopulations. Sorted cells were seeded at a density of 10 cells/cm² (for colony-forming and differentiation assays), or 50 cells/cm² (in case of subsequent long-term culture), and thereafter cultivated in growth medium at 3% O₂, 5% CO₂ and 37°C for further characterization. For immune fluorescence analysis, sorted cells were grown to near confluence and fixed with 4% *para*-formaldehyde / PBS for 10 min at ambient temperature. Actin filaments were stained with 1 μ g/ml Phalloidin-FITC (Sigma) in PBS for 30 min, and

nuclei were stained with 0.4 mM TO-PRO 3 (Molecular Probes) in PBS for 30 min at ambient temperature. Photographs were taken with the aid of an inverted Nikon Eclipse TE 300 fluorescence microscope equipped with a Nikon DigitalSight camera and a NIS Elements BR imaging software.

Statistics

Values were expressed as means \pm standard deviation of the mean; in the case of results shown in Fig 2, median \pm confidence interval ($p=0.05$) were shown.

Statistical differences of experimental scores were evaluated using Student's *t* tests.

Differences were considered significant when the *p* value was less than 0.05.

Results

As shown previously, MSC can be successfully isolated as a rare cell population from bone and bone marrow of differently aged individuals. When seeded *in vitro* as a low density culture, this cell type proliferates, thereby exhibiting clonogenic growth (19). Cultured at physiologic oxygen conditions (~3% O₂), MSC exhibit an enhanced proliferative capacity, while at the same time displaying a reduced differentiation potential (17).

Age-associated stem cell and differentiation potential of primary MSC

MSC were isolated from bone of healthy individuals of different age and both sexes (Supplementary Table 1). Clonogenic growth of plastic adherent, fibroblastoid cells was examined in low density cultures at atmospheric condition of 3% O₂ and 5% CO₂, and the number of colony-forming unit fibroblasts (CFU-f) was assessed (Figure 1). Individual results were grouped into four age classes: infants/teenager (0-20 years), young adults (20-40 years), aging adults (40-60 years) and seniors (60+). Thus, a decline in colony-forming ability between the young age groups and the seniors became apparent. In parallel, we also determined the differentiation potential of primary MSC regarding their osteogenic and adipogenic capacity by staining cultures three weeks after induction with lineage-specific histological dyes MSC derived from aged donors showed slightly elevated osteogenic potential, while the outcome of adipogenic differentiation was by and large equivalent between the four age groups (Supplementary Figure 1).

Mean telomere length of primary MSC

As the length of telomeres is thought to be a good indicator of the mitotic history of a cell (20-22), we monitored the mean length of telomeres of primary MSC, which had been derived from five young (9.1 ± 2.9 years) and six elderly individuals (62.3 ± 11.2 years), by means of quantitative reverse transcription PCR analysis (23). MSC from young donors displayed an average telomeric length of 11.6 ± 1.6 kbp, while telomeres in the older age group were only a little shorter, 10.4 ± 1.4 kbp (Supplementary Figure 2). This minor change was however found to be statistically insignificant ($p=0.95$).

Proliferation capacity of MSC in long-term culture

Next, we monitored the proliferative capacity of 30 primary MSC derived from differently aged persons of both sexes in long-term culture. For each individual line the maximum number of population doublings before reaching replicative senescence in culture was specified (Figure 1). The numbers of accumulated population doublings, were again evaluated by combining the results within the different age groups. An age-dependent decline was observed solely between cells derived from infants/teenagers and all adult groups.

Expression profiling of primary MSC from differently aged donors

In order to elucidate potential markers which are differentially expressed in MSC due to in vivo aging, primary cells from three young adults (22.7 ± 0.6 years) and three elderly donors (72.0 ± 5.3 years) were genomically analyzed. Prior to whole-genome expression profiling using Affymetrix Human Genome HG-133Plus 2.0 arrays, primary cells were subjected to short-term culture under normoxic conditions (3% O₂). The normalized data sets thereof were compared using an unsupervised method. Hierarchical clustering of about 20.000 probe sets which exhibited the

highest signal variance arranged the individual data sets according to donor ages (Supplementary Figure 3). This result demonstrated that potential candidate genes could be singled out. For selection criteria, a 1.5-fold difference in expression levels together with a p -value smaller than 0.05 was set in subsequent comparative analyses. This yielded a list of 288 probe sets corresponding to 225 genes that were upregulated in MSC derived from old donors, and 138 probe sets (118 genes) with lower expression levels in the aged group. When applying a more stringent cutoff of differential expression of greater than 2-fold, the number of probe sets/genes were 122/92 for upregulated transcripts and 26/20 with decreased expression in the aged group (for a list of differentially downregulated probe set IDs see Supplementary Tables 2; for upregulated probe set IDs see Supplementary Tables 3). To ease subsequent functional analyses, we next selected candidate genes that encode known cell surface molecules, for which specific antibodies are commercially available. To approve putative candidates their respective expression levels were assessed by means of quantitative reverse transcription-PCR in individual MSC derived from differently aged donors. Working along this line, only one upregulated gene was found differentially expressed in a highly reliable fashion. With high statistical significance, transcription of vascular cell adhesion molecule 1 (VCAM1, also called CD106) was elevated in MSC derived from persons of the older age groups (Figure 2).

Sorting of MSC according to VCAM1/CD106 levels

MSC were fractionated for further analyses by means of fluorescence-activated cell sorting according to VCAM1/CD106 levels (Figure 3). CD106^{dim} as well as CD106^{bright} cell fractions shared a high morphological microscopic resemblance. Colony-forming capacities after re-plating of CD106^{dim} and CD106^{bright} MSC were

comparable. Their respective proliferation potential after long-term cultivation and the corresponding growth characteristics exhibited only minor differences. In CD106^{bright} MSC an equally high transcript level with respect to stemness factors such as NANOG, REX1 or UTF1, the latter being controlled by SOX2 and OCT4 was found as in CD106^{dim} MSC; also no change in transcript levels of RUNX2, a transcription factor which is functionally involved in osteogenic lineage determination, as well as PPAR γ , a factor which defines adipogenic cell fate was observed. However when subjecting sorted MSC to differentiation regimens *in vitro*, CD106^{bright} MSC exhibited accelerated osteogenic lineage determination, while their adipogenic potential was diminished.

We further recognized that VCAM1 gene expression in MSC was stimulated by inflammatory cytokines, such as TNF α , or IFN γ . After treatment with increasing doses of IFN γ up to 100 units/mL, MSC derived from young and middle-aged donors showed a dose-dependent upregulation of both VCAM1 mRNA and the corresponding cell surface-bound CD106 protein product (Figure 4). In MSC from elderly donors, which already exhibited high levels of VCAM1 mRNA, this level remained constant, yet notably CD106 protein increased upon treatment with IFN γ . A 24 hour treatment with increasing doses of IFN γ neither had an impact on MSC colony-forming capacity nor influenced their viability (Suppl. Figure 5A). 10 units/mL IFN γ supplementation in long-term culture only slightly decreased MSC proliferation potential (Suppl. Figure 5B). Also, RUNX2, PPAR γ , REX1 and UTF1 expression levels remained by and large unchanged (Suppl. Figure 6).

Modulation of adipogenic and osteogenic differentiation potential of MSC

Next, we first primed MSC derived from a middle aged donor for three days with increasing doses of IFN γ before subjecting these cells to osteogenic or adipogenic differentiation *in vitro* in presence of IFN γ . The pre-treatment resulted in a dynamic modulation of both osteogenic and adipogenic differentiation *in vitro* (Figure 5). Osteogenesis-specific histological staining and molecular markers, such as osteopontin or osteocalcin were upregulated at low IFN γ concentration, while high doses of IFN γ abrogated osteogenic determination of MSC. In contrast to that, adipogenic differentiation potential was diminished with increasing IFN γ , yet at high doses of inflammatory stimuli, MSC showed enhanced adipogenic determination.

This experiment was replicated using primary cells from 4 donors of young to intermediate age (Figure 6). All individual MSC were first tested for multipotential differentiation capacity. The individual MSC lines showed a dose-dependent upregulation of CD106 upon IFN γ treatment, while at the same conditions, only a minute elevation of cell death could be examined (Suppl. Figure 5). Again with IFN γ supplementation the differentiation outcome could be modulated. However, the actual differentiation performance with respect to an osteogenic and adipogenic fate specification showed distinct age-dependent differences. MSC from young donors showed a tightly controlled response to increasing doses of IFN γ : very low concentrations of IFN γ greatly enhanced osteogenic marker expression, while higher doses (>10 units/mL) actually depressed their osteogenic differentiation potential. Adipogenic fate was impacted in a similar fashion; notably however, at high IFN γ doses marker expression remained at levels comparable to unstimulated controls. In contrast, MSC from middle-aged adults, which express elevated levels of CD106, only showed enhanced osteogenic marker expression with IFN γ supplementation higher than 10 units/mL; yet when being differentiated under the same conditions,

adipogenic determination appeared to be depressed. At high doses of up to 100 units/mL of IFN γ , both osteogenic and adipogenic differentiation potential was at levels comparable to unstimulated controls.

Next we iterated the experiment, now employing MSC with proven multipotentiality, self renewal capacity and CD106 upregulation upon stimulation with IFN γ , which had been isolated from healthy elderly donors of an advanced age of 80 years (Figure 7). These MSC lines also showed a dose-dependent upregulation of CD106 upon IFN γ treatment, although the increase was only slight. This treatment only resulted in a minute elevation of cell death (data not shown). The osteogenic differentiation capacity of these cells was greatly diminished in response to any dose of IFN γ supplementation. This phenomenon was evidenced using several markers, which were found suitable for grading osteogenic fate decision before, such as osteopontin, osteocalcin, bone sialoprotein II, alkaline phosphatase or osteonectin. Although adipogenic differentiation also showed dynamic changes under the conditions applied, a downregulation as distinct as examined for osteogenic determination could not be observed, and cells unaffectedly underwent adipogenic differentiation when simultaneously being provoked by an inflammatory environment.

Discussion

Tissue homeostasis, regeneration and repair require the emergence and integration of new parenchymal cells descending from undifferentiated cells. The latter are resident in many, albeit not all body organs and tissues. Hence, a decline of stem cell function and activity with advancing age contributes to a delayed replacement and turnover of damaged cells in compromised renewable tissues, such as muscle, bone, intestine or skin. The efficiency of tissue regeneration processes is influenced by stem cell-intrinsic factors, yet certainly is also geared by extrinsic determinants and signals, both of which are subject to change with advancing age (24). This in mind, work has focused in scrutinizing the exact number of tissue-specific stem cells together with their respective quality. MSC can be selected from mononuclear cell isolates based on their characteristic trait of tightly adhering to the plastic surface of the culture dish, and there to initiate the growth of fibroblastic colonies. The respective number, also called colony-forming unit-fibroblast, or CFU-f, can be reliably estimated. Applying this method, there are conflicting results regarding the respective MSC number changes during life span. Some laboratories report that total CFU-f decrease with age (11,25-29), others find stable numbers (30-35). A particular problem with this type of approach is that there is no agreement on a single, standardized protocol for the isolation and subsequent analysis of primary MSC. In addition, primary cell isolates also contain other cells, in particular hematopoietic cells, which may compromise colony formation or disturb self-renewal properties of MSC. These limitations did not dissuade us from also surveying the CFU-f capacity in primary MSC cultures from 29 donors of different age. In parallel, the same cultures were grown and stimulated to further differentiate in order to assess the individual osteogenic and adipogenic potential. Unexpectedly, primary MSC isolated from donors of advancing age exhibited enhanced osteogenic potential, whereas the

adipogenic capacity appeared comparable throughout age groups. This peculiar unexpected phenotypic appearance *in vitro* has also been noticed by others (36).

Assignment of age-specific MSC markers

In vitro, the proliferative capacity of primary mammalian cells is finite (37). After extensive expansion, also cultured human MSC cease growth and enter a state of irreversible growth arrest, referred to as “replicative senescence” (13,14,38). When growing MSC in long-term culture, we recognized, similarly to what has been reported by others (29,36,39) that the number of population doublings accumulated by MSC lines derived from individual donors varies considerably. Besides unique basic MSC markers and well-defined *in vivo* assays, no specific and reliable biomarker for MSC-intrinsic aging is available to date. This circumstance further restricts our understanding of biological processes accompanying or bringing forth MSC aging. Above all, another important purpose in the scope of this research is to establish efficient means for tagging abnormal, aged or senescent MSC as a prerequisite to eliminate the risk patients are facing when being treated with MSC (16).

We approached these problems by comparing whole genome gene expression profiles of primary MSC from differently aged, healthy individuals. We primarily concentrated on differentially expressed genes which encode known proteins that are presented at the outer cell surface (40); suffice it to say that antibodies which are commercially available to detect such factors would ease any subsequent functional characterization. One of the candidates emerging from the wealth of genomic data was VCAM1/CD106. This cell surface molecule has often been considered a valid MSC marker, yet conspicuously exhibiting a non-uniform expression level (41-48). CD106 has also been found to be expressed on murine (49) and rat MSC (50).

However MSC derived from umbilical cord are either void of CD106 (51), or it is expressed only at very low levels (52). Similarly, adipose-derived MSC bear sparse amounts of CD106 (53). We found this marker differentially expressed in primary MSC derived from bone of differently aged donors, both at transcript and protein level. We also recognized that there is a high variability of expression between individual samples, in particular within the older age groups. Proliferation and self-renewal assays as well as quantitative assessment of the levels of various transcription factors involved in the regulation and control of stemness and differentiation indicated that regardless of CD106 expression, MSC exhibited no apparent difference. CD106/VCAM-1 specifically interacts with members of the integrin family such as alpha4/beta7 integrin and it is well documented that binding activates integrin signalling (54). Up to now it is still unknown whether integrin signaling regulates the multipotentiality of MSC.

“Inflamm-aging” of MSC

VCAM1 expression in endothelial cells is strongly enhanced by pro-inflammatory cytokines. In MSC, IFN γ or TNF α activate VCAM1 expression. Besides VCAM1, our array analysis also revealed other genes, which are potentially upregulated by inflammatory cytokines, namely CCL2, IFIT1, and SOD2. In human foreskin fibroblasts these genes are strongly upregulated after IFN γ stimulation (55). In endothelial HMEC4 cells treated with TNF α , not only the expected VCAM1 gene, yet also the expression of these three genes could be enhanced (56). CCL2 is also significantly upregulated in human MSC upon IFN γ treatment (57). TNFRSF10B (TRAIL-R2, which is upregulated in mouse embryonic fibroblasts by TNF-alpha through NF κ B-dependent signaling (58), and PAPPA which is induced by TNF-alpha

and IL1-beta in human dermal fibroblasts (59) are further genes which we also unveiled in aged MSC being transcribed at significantly higher levels.

Prominent sources of pro-inflammatory cytokines such as IFN γ are T lymphocytes and NK cells. In the last few years, it became clear that MSC exhibit immune regulatory properties (60). MSC not only passively withstand inflammatory stimuli, but more than that, MSC decisively respond to inflammatory cues, e.g. by promoting the expression of indoleamine 2,3-dioxygenase, which leads to tryptophan depletion in lymphocytes, and thus modulates lymphocyte activity and proliferation (61). As shown in this contribution, IFN γ also exerts its effect on MSC commitment with regard to distinct lineage-specific differentiation capacity. The proliferative potential however appeared to be not impacted. Interesting in this context are contradicting reports demonstrating that the differentiation potential of CD106 positive MSC is clearly osteogenic (62), while in stark contrast, CD106⁺ MSC were reported to be prone to the adipogenic lineage (63). This data incongruence can be reconciled by our results.

In turn, dominant aberrations within the MSC microenvironment may arise from systemic chronic inflammation as described to occur regularly in elderly persons, or unbalanced inflammatory and anti-inflammatory networks as a consequence to life-long antigenic burden or age-related diseases (15). In accordance to that assumption, a high prevalence of osteopenic pathology is being associated with chronic inflammatory syndroms such as Crohn's disease or ulcerative colitis, cystic fibrosis, nephritis, vasculitis and inflammatory neuropathies (64).

It is less appreciated that inflammation negatively impacts on osteoblastogenesis (65) and more than that as also shown in this contribution that osteogenic lineage progenitor cells become sustainingly altered by an inflammatory milieu. Wagner and colleagues only recently reported epigenetic changes of MSC upon aging and noted

differential DNA methylation pattern in gene loci of the interferon-gamma receptor beta chain, the interleukin 1 receptor antagonist isoform 3, or the suppressor of cytokine signaling 1, as well as factors related to TNF-signaling such as RIPK1, TNFSF4, TNFRSF10C, TNFSF13B, TNFAIP2 and TNFSF4 (66). In line with this, age-related intrinsic alterations in human bone marrow-derived MSC with respect to osteogenic differentiation potential (35) and loss of osteogenic capacity as a result of enhanced adipogenic determination have been documented (67). Imbalanced inflammatory cues are thus furthermore leading to a likely deviation from properly guiding molecular signaling mechanisms during regeneration, repair and tissue remodeling (68), and may thus gear a pronounced impetus for adipogenic upgrowth, as a well-known example, bone marrow adipositas. In addition to that we could further show here that advancedly aged MSC are prone to greatly loose bearings with respect to osteogenesis in an inflammatory environment.

Conclusion

The ontological and anatomical origins of MSC have a profound influence on individual MSC's differentiation capacity: Early in life, most uncommitted MSC exhibit multipotential differentiation capacity, and their developmental fate is tightly controlled. Later in life however, additional characters of mesenchymal precursors may emerge. We found VCAM-1 levels considerably increased in MSC of elderly donors. MSC appear to be greatly responsive to pro-inflammatory cytokines such as TNF α or IFN γ , which upregulate VCAM-1 expression. As a consequence, these cells become committed to either differentiate towards the adipogenic or osteogenic lineage. Conclusively, a rise in VCAM1/CD106 expression is indicative for alterations of MSC stemness. Our results further indicate that excessive or chronic inflammatory insults in later life may actually promote adipogenic differentiation and adipose

upgrowth. Moreover, CD106 also appears to be a suitable marker of clinical relevance, in particular for the assessment of allostatic load on MSC concerning environmental stress, such as exuberantly fluctuating inflammatory cues.

Taken together, our observations suggest that according to defined environmental specifications, VCAM1/CD106 is upregulated in MSC which commit themselves to lineage-specific differentiation: at young age, elevated, yet well adjusted levels of inflammatory stimuli which are known to go along with wound and bone healing are able to support osteoblastogenesis; lack of this type of instructive signal would rather favor adipogenic differentiation.

Acknowledgements

This work was supported by the Austrian Science Fund (FWF) through a National Research Network grant (NRN 093 05) and by the Jubilee Fund of the Austrian National Bank (#12518). We are particularly indebted to Brigitte Greiderer for her professional help and technical assistance.

Author contribution

GTL: collection and assembly of data, data analysis and interpretation, final approval of manuscript

RB: collection and assembly of data, data analysis and interpretation, final approval of manuscript

AJ: collection of data

CF: collection of data

SS: collection of data

HH: collection of data

FK: provision of study material or patients, final approval of manuscript

RG: provision of study material or patients, final approval of manuscript

GL: conception and design, data analysis and interpretation, financial support, administrative support, manuscript writing

Competing interest statement

The authors declare that they have no competing financial interests or others that might perceive to influence the results and discussion reported in this paper

References

1. Caplan AI 1991 Mesenchymal stem cells. *J Orthop Res* **9**(5):641-50.
2. Horwitz EM, Le Blanc K, Dominici M, Mueller I, Slaper-Cortenbach I, Marini FC, Deans RJ, Krause DS, Keating A 2005 Clarification of the nomenclature for MSC: The International Society for Cellular Therapy position statement. *Cytotherapy* **7**(5):393-5.
3. Caplan AI 2009 Why are MSCs therapeutic? New data: new insight. *J Pathol* **217**(2):318-24.
4. Abdallah BM, Kassem M 2009 The use of mesenchymal (skeletal) stem cells for treatment of degenerative diseases: current status and future perspectives. *J Cell Physiol* **218**(1):9-12.
5. Phinney DG, Prockop DJ 2007 Concise review: mesenchymal stem/multipotent stromal cells: the state of transdifferentiation and modes of tissue repair--current views. *Stem Cells* **25**(11):2896-902.
6. Uccelli A, Moretta L, Pistoia V 2008 Mesenchymal stem cells in health and disease. *Nat Rev Immunol* **8**(9):726-36.
7. Pittenger MF, Mosca JD, McIntosh KR 2000 Human mesenchymal stem cells: progenitor cells for cartilage, bone, fat and stroma. *Curr Top Microbiol Immunol* **251**:3-11.
8. Gronthos S, Graves SE, Ohta S, Simmons PJ 1994 The STRO-1+ fraction of adult human bone marrow contains the osteogenic precursors. *Blood* **84**(12):4164-73.
9. Horwitz EM, Keating A 2000 Nonhematopoietic mesenchymal stem cells: what are they? *Cytotherapy* **2**(5):387-8.
10. Prockop DJ, Sekiya I, Colter DC 2001 Isolation and characterization of rapidly self-renewing stem cells from cultures of human marrow stromal cells. *Cytotherapy* **3**(5):393-6.
11. Caplan AI 2007 Adult mesenchymal stem cells for tissue engineering versus regenerative medicine. *J Cell Physiol* **213**(2):341-7.
12. Lepperdinger G 2008 Aging stem cells and regenerative biomedicine: concepts, opportunities and technological advances. *Exp Gerontol* **43**(11):967.
13. Fehrer C, Lepperdinger G 2005 Mesenchymal stem cell aging. *Exp Gerontol* **40**(12):926-30.

14. Sethe S, Scutt A, Stolzing A 2006 Aging of mesenchymal stem cells. *Ageing Res Rev* **5**(1):91-116.
15. Franceschi C, Capri M, Monti D, Giunta S, Olivieri F, Sevini F, Panourgia MP, Invidia L, Celani L, Scurti M, Cevenini E, Castellani GC, Salvioli S 2007 Inflammaging and anti-inflammaging: a systemic perspective on aging and longevity emerged from studies in humans. *Mech Ageing Dev* **128**(1):92-105.
16. Lepperdinger G, Brunauer R, Jamnig A, Laschober G, Kassem M 2008 Controversial issue: is it safe to employ mesenchymal stem cells in cell-based therapies? *Exp Gerontol* **43**(11):1018-23.
17. Fehrer C, Brunauer R, Laschober G, Unterluggauer H, Reitingner S, Kloss F, Gully C, Gassner R, Lepperdinger G 2007 Reduced oxygen tension attenuates differentiation capacity of human mesenchymal stem cells and prolongs their lifespan. *Aging Cell* **6**(6):745-57.
18. Rainer J, Sanchez-Cabo F, Stocker G, Sturn A, Trajanoski Z 2006 CARMAweb: comprehensive R- and bioconductor-based web service for microarray data analysis. *Nucleic Acids Res* **34**(Web Server issue):W498-503.
19. Prockop DJ 1997 Marrow stromal cells as stem cells for nonhematopoietic tissues. *Science* **276**(5309):71-4.
20. Davis T, Skinner JW, Faragher RG, Jones CJ, Kipling D 2005 Replicative senescence in sheep fibroblasts is a p53 dependent process. *Exp Gerontol* **40**(1-2):17-26.
21. Effros RB, Dagarag M, Valenzuela HF 2003 In vitro senescence of immune cells. *Exp Gerontol* **38**(11-12):1243-9.
22. von Zglinicki T, Martin-Ruiz CM 2005 Telomeres as biomarkers for ageing and age-related diseases. *Curr Mol Med* **5**(2):197-203.
23. Fehrer C, Voglauer R, Wieser M, Pfister G, Brunauer R, Cioca D, Grubeck-Loebenstien B, Lepperdinger G 2006 Techniques in gerontology: cell lines as standards for telomere length and telomerase activity assessment. *Exp Gerontol* **41**(6):648-51.
24. Rando TA 2006 Stem cells, ageing and the quest for immortality. *Nature* **441**(7097):1080-6.
25. Baxter MA, Wynn RF, Jowitt SN, Wraith JE, Fairbairn LJ, Bellantuono I 2004 Study of telomere length reveals rapid aging of human marrow stromal cells following in vitro expansion. *Stem Cells* **22**(5):675-82.

26. Majors AK, Boehm CA, Nitto H, Midura RJ, Muschler GF 1997 Characterization of human bone marrow stromal cells with respect to osteoblastic differentiation. *J Orthop Res* **15**(4):546-57.
27. Muschler GF, Nitto H, Boehm CA, Easley KA 2001 Age- and gender-related changes in the cellularity of human bone marrow and the prevalence of osteoblastic progenitors. *J Orthop Res* **19**(1):117-25.
28. Nishida S, Endo N, Yamagiwa H, Tanizawa T, Takahashi HE 1999 Number of osteoprogenitor cells in human bone marrow markedly decreases after skeletal maturation. *J Bone Miner Metab* **17**(3):171-7.
29. Stolzing A, Jones E, McGonagle D, Scutt A 2008 Age-related changes in human bone marrow-derived mesenchymal stem cells: consequences for cell therapies. *Mech Ageing Dev* **129**(3):163-73.
30. D'Ippolito G, Schiller PC, Ricordi C, Roos BA, Howard GA 1999 Age-related osteogenic potential of mesenchymal stromal stem cells from human vertebral bone marrow. *J Bone Miner Res* **14**(7):1115-22.
31. Glowacki J 1995 Influence of age on human marrow. *Calcif Tissue Int* **56 Suppl 1**:S50-1.
32. Justesen J, Stenderup K, Eriksen EF, Kassem M 2002 Maintenance of osteoblastic and adipocytic differentiation potential with age and osteoporosis in human marrow stromal cell cultures. *Calcif Tissue Int* **71**(1):36-44.
33. Oreffo RO, Bennett A, Carr AJ, Triffitt JT 1998 Patients with primary osteoarthritis show no change with ageing in the number of osteogenic precursors. *Scand J Rheumatol* **27**(6):415-24.
34. Stenderup K, Justesen J, Eriksen EF, Rattan SI, Kassem M 2001 Number and proliferative capacity of osteogenic stem cells are maintained during aging and in patients with osteoporosis. *J Bone Miner Res* **16**(6):1120-9.
35. Zhou S, Greenberger JS, Epperly MW, Goff JP, Adler C, Leboff MS, Glowacki J 2008 Age-related intrinsic changes in human bone-marrow-derived mesenchymal stem cells and their differentiation to osteoblasts. *Aging Cell* **7**(3):335-43.
36. Wagner W, Horn P, Castoldi M, Diehlmann A, Bork S, Saffrich R, Benes V, Blake J, Pfister S, Eckstein V, Ho AD 2008 Replicative senescence of mesenchymal stem cells: a continuous and organized process. *PLoS ONE* **3**(5):e2213.

37. Hayflick L 1965 The Limited in Vitro Lifetime of Human Diploid Cell Strains. *Exp Cell Res* **37**:614-36.
38. Beausejour C 2007 Bone marrow-derived cells: the influence of aging and cellular senescence. *Handb Exp Pharmacol* (180):67-88.
39. Shibata KR, Aoyama T, Shima Y, Fukiage K, Otsuka S, Furu M, Kohno Y, Ito K, Fujibayashi S, Neo M, Nakayama T, Nakamura T, Toguchida J 2007 Expression of the p16INK4A gene is associated closely with senescence of human mesenchymal stem cells and is potentially silenced by DNA methylation during in vitro expansion. *Stem Cells* **25**(9):2371-82.
40. Laschober GT, Brunauer R, Jamnig A, Fehrer C, Greiderer B, Lepperdinger G 2009 Leptin receptor/CD295 is upregulated on primary human mesenchymal stem cells of advancing biological age and distinctly marks the subpopulation of dying cells. *Exp Gerontol* **44**(1-2):57-62.
41. Sarugaser R, Lickorish D, Baksh D, Hosseini MM, Davies JE 2005 Human umbilical cord perivascular (HUCPV) cells: a source of mesenchymal progenitors. *Stem Cells* **23**(2):220-9.
42. Lupatov AY, Karalkin PA, Suzdal'tseva YG, Burunova VV, Yarygin VN, Yarygin KN 2006 Cytofluorometric analysis of phenotypes of human bone marrow and umbilical fibroblast-like cells. *Bull Exp Biol Med* **142**(4):521-6.
43. Gronthos S, Zannettino AC, Hay SJ, Shi S, Graves SE, Kortessidis A, Simmons PJ 2003 Molecular and cellular characterisation of highly purified stromal stem cells derived from human bone marrow. *J Cell Sci* **116**(Pt 9):1827-35.
44. Wagner W, Wein F, Seckinger A, Frankhauser M, Wirkner U, Krause U, Blake J, Schwager C, Eckstein V, Ansorge W, Ho AD 2005 Comparative characteristics of mesenchymal stem cells from human bone marrow, adipose tissue, and umbilical cord blood. *Exp Hematol* **33**(11):1402-16.
45. Pittenger MF, Mackay AM, Beck SC, Jaiswal RK, Douglas R, Mosca JD, Moorman MA, Simonetti DW, Craig S, Marshak DR 1999 Multilineage potential of adult human mesenchymal stem cells. *Science* **284**(5411):143-7.
46. Tuli R, Tuli S, Nandi S, Wang ML, Alexander PG, Haleem-Smith H, Hozack WJ, Manner PA, Danielson KG, Tuan RS 2003 Characterization of multipotential mesenchymal progenitor cells derived from human trabecular bone. *Stem Cells* **21**(6):681-93.

47. Gronthos S, Franklin DM, Leddy HA, Robey PG, Storms RW, Gimble JM 2001 Surface protein characterization of human adipose tissue-derived stromal cells. *J Cell Physiol* **189**(1):54-63.
48. Jones EA, English A, Kinsey SE, Straszynski L, Emery P, Ponchel F, McGonagle D 2006 Optimization of a flow cytometry-based protocol for detection and phenotypic characterization of multipotent mesenchymal stromal cells from human bone marrow. *Cytometry B Clin Cytom* **70**(6):391-9.
49. Peister A, Mellad JA, Larson BL, Hall BM, Gibson LF, Prockop DJ 2004 Adult stem cells from bone marrow (MSCs) isolated from different strains of inbred mice vary in surface epitopes, rates of proliferation, and differentiation potential. *Blood* **103**(5):1662-8.
50. Tokalov SV, Gruner S, Schindler S, Wolf G, Baumann M, Abolmaali N 2007 Age-related changes in the frequency of mesenchymal stem cells in the bone marrow of rats. *Stem Cells Dev* **16**(3):439-46.
51. Kogler G, Sensken S, Airey JA, Trapp T, Muschen M, Feldhahn N, Liedtke S, Sorg RV, Fischer J, Rosenbaum C, Greschat S, Knipper A, Bender J, Degistirici O, Gao J, Caplan AI, Colletti EJ, Almeida-Porada G, Muller HW, Zanjani E, Wernet P 2004 A new human somatic stem cell from placental cord blood with intrinsic pluripotent differentiation potential. *J Exp Med* **200**(2):123-35.
52. Lu LL, Liu YJ, Yang SG, Zhao QJ, Wang X, Gong W, Han ZB, Xu ZS, Lu YX, Liu D, Chen ZZ, Han ZC 2006 Isolation and characterization of human umbilical cord mesenchymal stem cells with hematopoiesis-supportive function and other potentials. *Haematologica* **91**(8):1017-26.
53. Zuk PA, Zhu M, Ashjian P, De Ugarte DA, Huang JI, Mizuno H, Alfonso ZC, Fraser JK, Benhaim P, Hedrick MH 2002 Human adipose tissue is a source of multipotent stem cells. *Mol Biol Cell* **13**(12):4279-95.
54. Lobb RR, Hemler ME 1994 The pathophysiologic role of alpha 4 integrins in vivo. *J Clin Invest* **94**(5):1722-8.
55. Kim SK, Fouts AE, Boothroyd JC 2007 *Toxoplasma gondii* dysregulates IFN-gamma-inducible gene expression in human fibroblasts: insights from a genome-wide transcriptional profiling. *J Immunol* **178**(8):5154-65.
56. Valencia JV, Mone M, Zhang J, Weetall M, Buxton FP, Hughes TE 2004 Divergent pathways of gene expression are activated by the RAGE ligands S100b and AGE-BSA. *Diabetes* **53**(3):743-51.

57. Romieu-Mourez R, Francois M, Boivin MN, Bouchentouf M, Spaner DE, Galipeau J 2009 Cytokine modulation of TLR expression and activation in mesenchymal stromal cells leads to a proinflammatory phenotype. *J Immunol* **182**(12):7963-73.
58. Ravi R, Bedi GC, Engstrom LW, Zeng Q, Mookerjee B, Gelinas C, Fuchs EJ, Bedi A 2001 Regulation of death receptor expression and TRAIL/Apo2L-induced apoptosis by NF-kappaB. *Nat Cell Biol* **3**(4):409-16.
59. Resch ZT, Chen BK, Bale LK, Oxvig C, Overgaard MT, Conover CA 2004 Pregnancy-associated plasma protein a gene expression as a target of inflammatory cytokines. *Endocrinology* **145**(3):1124-9.
60. Dazzi F, Ramasamy R, Glennie S, Jones SP, Roberts I 2006 The role of mesenchymal stem cells in haemopoiesis. *Blood Rev* **20**(3):161-71.
61. Frumento G, Rotondo R, Tonetti M, Damonte G, Benatti U, Ferrara GB 2002 Tryptophan-derived catabolites are responsible for inhibition of T and natural killer cell proliferation induced by indoleamine 2,3-dioxygenase. *J Exp Med* **196**(4):459-68.
62. Fukiage K, Aoyama T, Shibata KR, Otsuka S, Furu M, Kohno Y, Ito K, Jin Y, Fujita S, Fujibayashi S, Neo M, Nakayama T, Nakamura T, Toguchida J 2008 Expression of vascular cell adhesion molecule-1 indicates the differentiation potential of human bone marrow stromal cells. *Biochem Biophys Res Commun* **365**(3):406-12.
63. Liu F, Akiyama Y, Tai S, Maruyama K, Kawaguchi Y, Muramatsu K, Yamaguchi K 2008 Changes in the expression of CD106, osteogenic genes, and transcription factors involved in the osteogenic differentiation of human bone marrow mesenchymal stem cells. *J Bone Miner Metab* **26**(4):312-20.
64. Hardy R, Cooper MS 2009 Bone loss in inflammatory disorders. *J Endocrinol* **201**(3):309-20.
65. Petitpain N, Gambier N, Wahl D, Chary-Valckenaere I, Loeuille D, Gillet P 2009 Arterial and venous thromboembolic events during anti-TNF therapy: a study of 85 spontaneous reports in the period 2000-2006. *Biomed Mater Eng* **19**(4-5):355-64.
66. Bork S, Pfister S, Witt H, Horn P, Korn B, Ho AD, Wagner W DNA methylation pattern changes upon long-term culture and aging of human mesenchymal stromal cells. *Aging Cell* **9**(1):54-63.

67. Moerman EJ, Teng K, Lipschitz DA, Lecka-Czernik B 2004 Aging activates adipogenic and suppresses osteogenic programs in mesenchymal marrow stroma/stem cells: the role of PPAR-gamma2 transcription factor and TGF-beta/BMP signaling pathways. *Aging Cell* **3**(6):379-89.
68. Cartwright MJ, Tchkonina T, Kirkland JL 2007 Aging in adipocytes: potential impact of inherent, depot-specific mechanisms. *Exp Gerontol* **42**(6):463-71.

Figure Legends

Figure 1: Properties of primary MSCs derived from differently aged healthy individuals.

(A) Primary colony forming units-fibroblasts (pCFU-f) grown from 29 mononuclear cell (MNC) preparations derived from bone biopsies of healthy individuals; (B) the individual results thereof were pooled according to four age groups (<20, 20-40, 40-60 and >60 years) and statistically evaluated.

Long-term cultures of primary MSC. (C-F) MSC isolated from bone biopsies of 30 differently aged healthy individuals (female: circles; males: squares). Cultures were propagated as low density cultures, and accumulation of population doublings was documented over time. (A) Long-term growth kinetics of MSC from young (below 20 years), (B) young adults (20-40 years), (C) middle aged (40-60 years), and old individuals (above 60 years) (D) are depicted. Cumulative population doublings (CPD) before reaching irreversible growth arrest were accounted and plotted versus donor age (G) and further statistically validated (H).

Figure 2: VCAM1 expression levels in primary MSC.

(A) VCAM1 transcript levels in primary MSC derived from differently aged, healthy individuals; in detail, 7 infant/teenage donors (9.8 +/- 2.7 years), 9 young adults (27.1 +/- 5.9 years), 9 aged adults (50.8 +/- 3.1 years), and 9 seniors (69.0 +/- 7.4 years).

Figure 3: MSC bearing high or low amounts of CD106 antigen.

MSC were separated from dying cells by staining with annexinV. Living cells were further sorted for subsets expressing high levels of CD106 (VCAM^{bright}) and those only presenting minute amounts of CD106 on their surface (VCAM^{dim}). (A) Fluorescence-activated cell sorting of MSC with respect to VCAM1 levels: MSC were separated from dying cells stained with annexinV; the remaining cells were further sorted for subsets

expressing high levels of CD106 (VCAM^{bright}) and those only presenting minute amounts of CD106 (VCAM^{dim}): MSC before FACS – black line, isotype control – grey histogram, VCAM^{bright} – red histogram, VCAM^{dim} - blue histogram; (B) micrographs of cells stained with FITC phalloidin to label the actin cytoskeleton and TO-PRO 3 to highlight the cell nucleus; scale bar is 100 μ m. (C) colony-forming capacity in cell populations sorted according to CD106 surface expression; (D) representative example of the respective proliferative capacity in long-term cultures of VCAM^{bright} and VCAM^{dim} MSC (E) relative transcriptional activities of VCAM^{bright} over that of VCAM^{dim} MSC (n=7) with respect to VCAM1, the stemness associated transcription factors NANOG, REX1 and UTF1, as well as the osteogenic and adipogenic specific transcription factors RUNX2 and PPAR γ measured by quantitative reverse transcription-PCR; (F) relative expression levels of osteogenesis and adipogenesis-specific markers comparing VCAM^{bright} over that of VCAM^{dim} MSC after 3 weeks of differentiation *in vitro*.

Figure 4: MSC under inflammatory stress. VCAM1 mRNA and CD106 expression levels in MSC derived from three healthy individuals (donor age as indicated), which had been cultured in the presence of increasing concentrations of interferon gamma (IFN γ) for 24 hours.

Figure 5: Osteogenic and adipogenic differentiation in the presence of increasing doses of IFN γ . (A) Histological evaluation of *in vitro* osteogenic (alizarin red) together with assessment of osteogenic lineage markers, osteopontin (SPP1) and osteocalcin (PMF1); (B) Histological evaluation of adipogenic (oil red) differentiation potential together with transcript levels of adipogenic lineage markers, fatty acid binding protein 4 (FABP4) and lipoprotein lipase (LPL). Measurements were performed in triplicates by quantitative reverse transcription-PCR.

Figure 6: Modulation of bilineage differentiation capacity by interferon gamma in MSC derived from young and intermediately aged individuals. Osteogenic and adipogenic marker profiles of MSC isolated from healthy donors of different age as indicated. The cells were differentiated in vitro in the presence of raising doses of IFN γ as indicated. Measurements were performed in triplicates by quantitative reverse transcription-PCR.

Figure 7: Differentiation of MSC derived from elderly individuals. Osteogenic and adipogenic marker profiles of MSC from two 80-year old donors. Cells were subjected to in vitro differentiation in the presence of increasing doses of IFN γ . Transcript numbers of various differentiation-specific marker were assessed in triplicates by quantitative reverse transcription-PCR; osteogenic lineage markers were osteopontin (SPP1), osteocalcin (PMF1), alkaline phosphatase (ALP), bone sialo protein II (IBSP) and osteonectin (SPARC); adipogenic lineage marker: fatty acid binding protein 4 (FABP4).

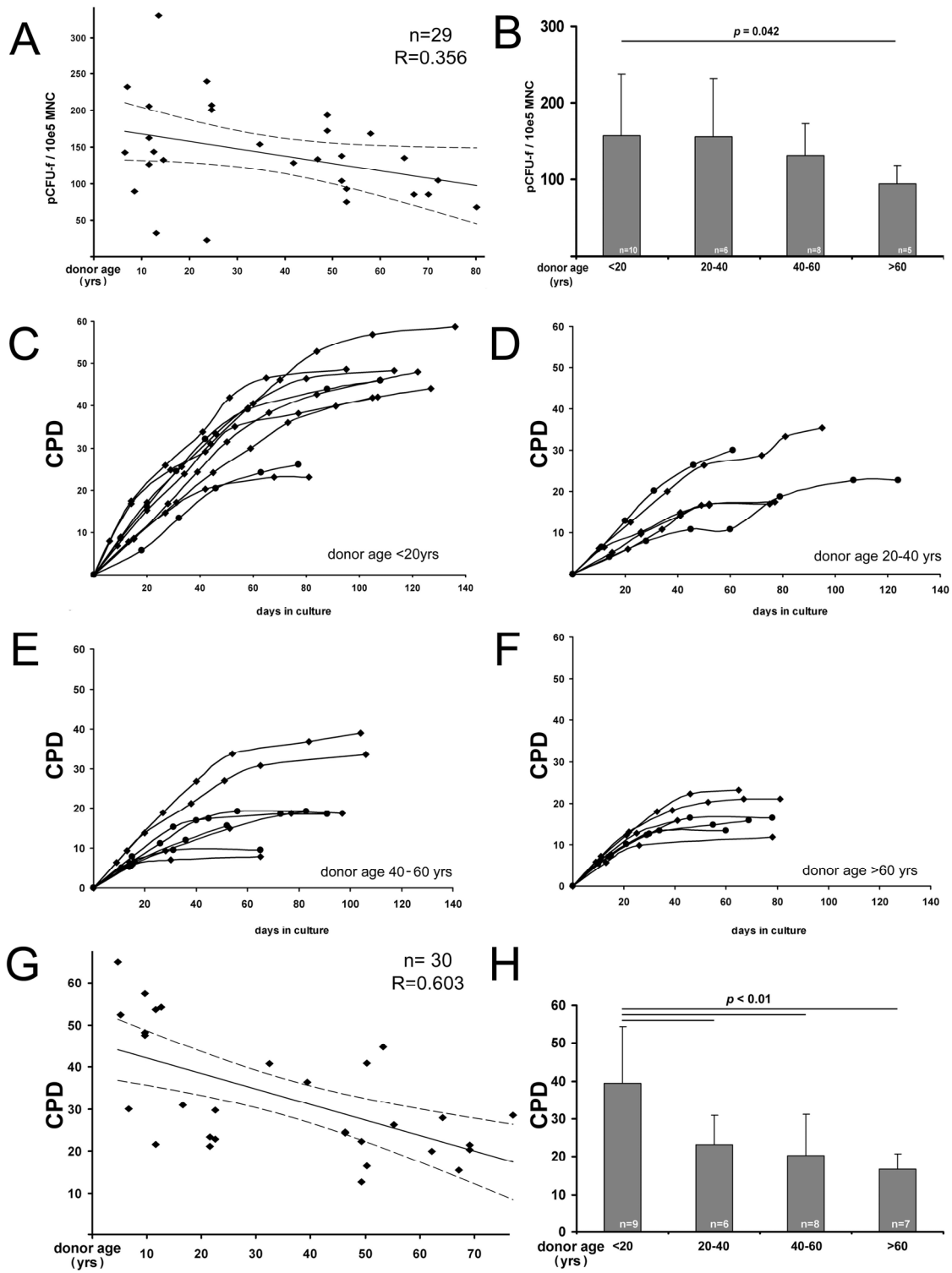


Figure 1

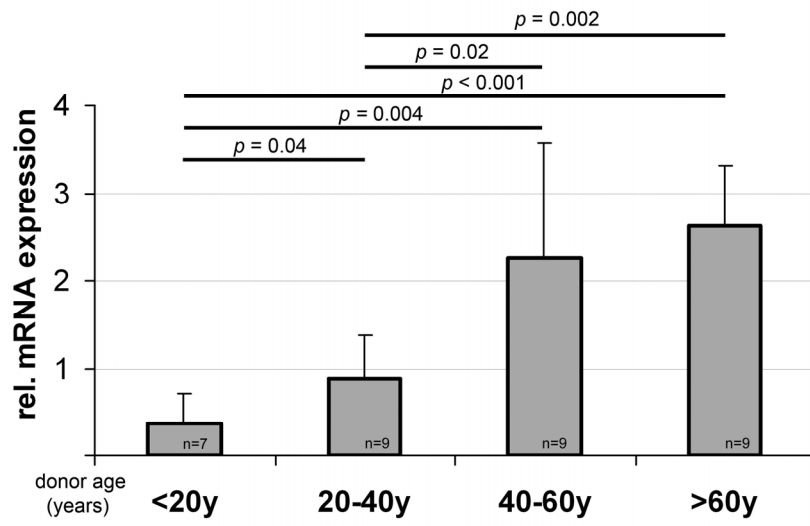


Figure 2

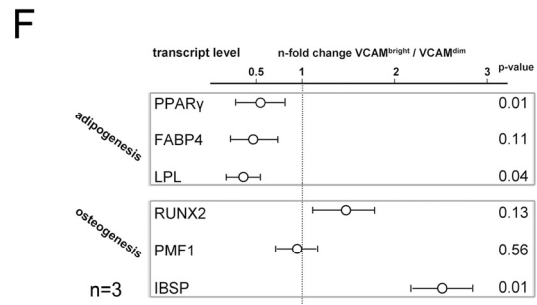
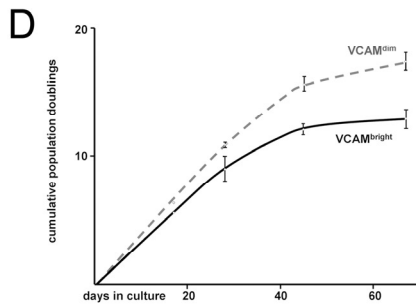
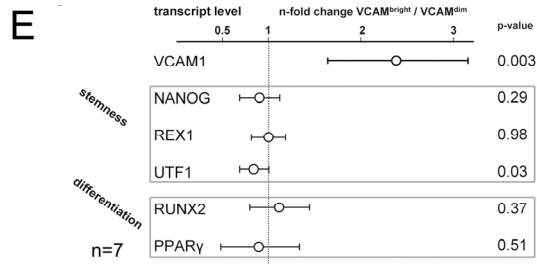
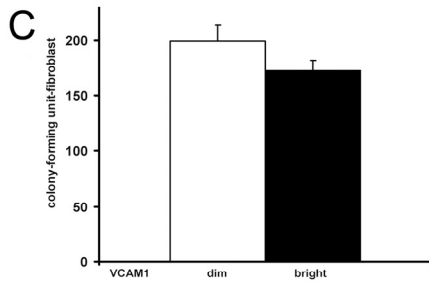
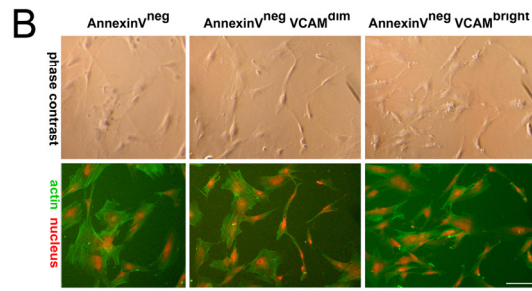
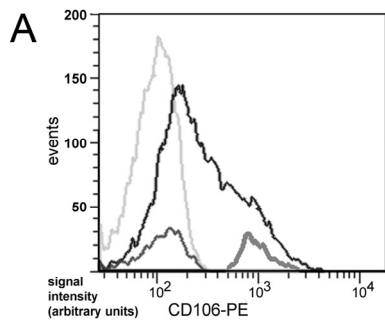


Figure 3

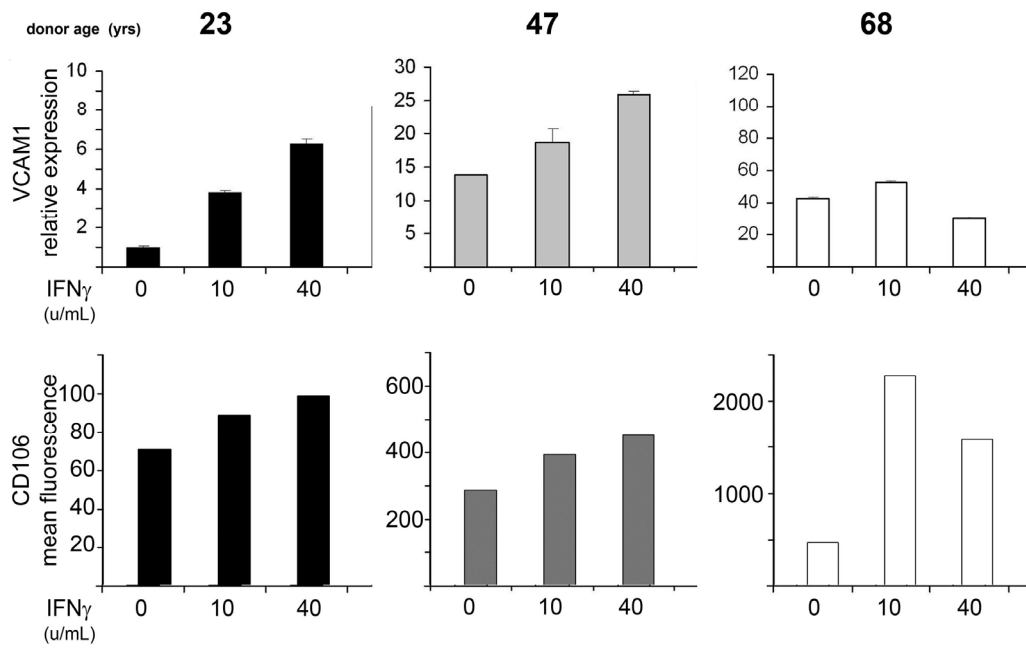


Figure 4

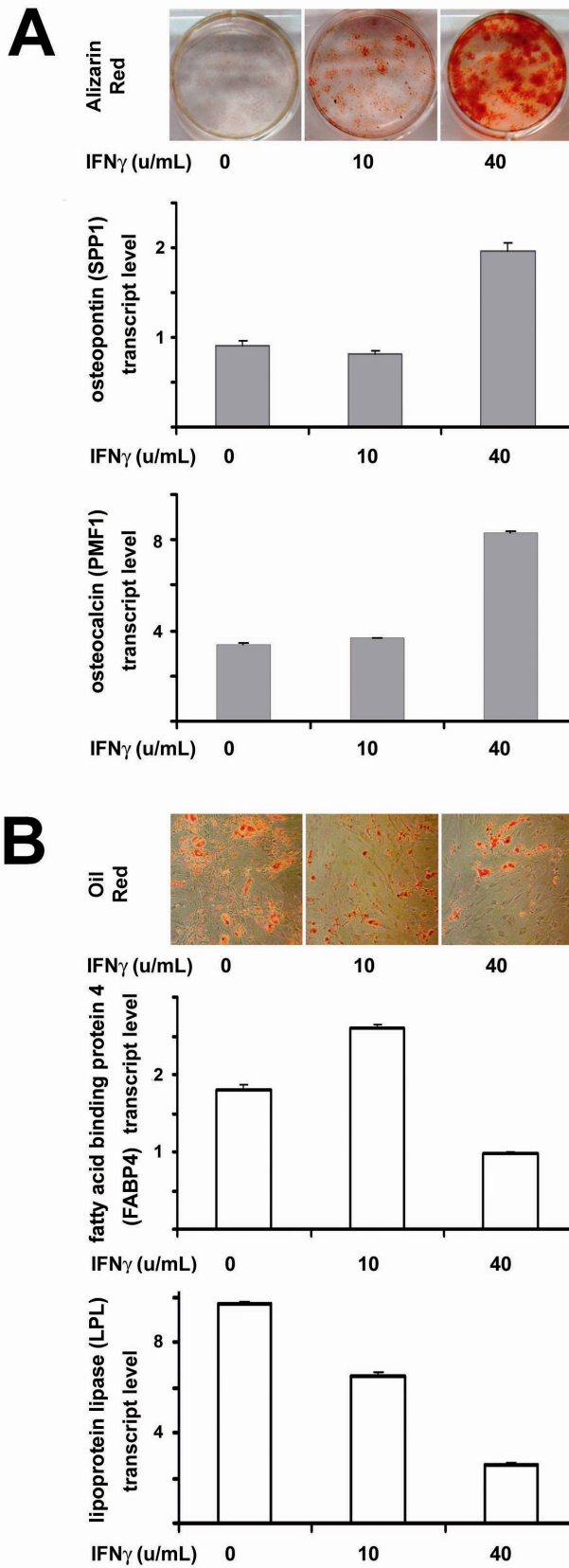


Figure 5

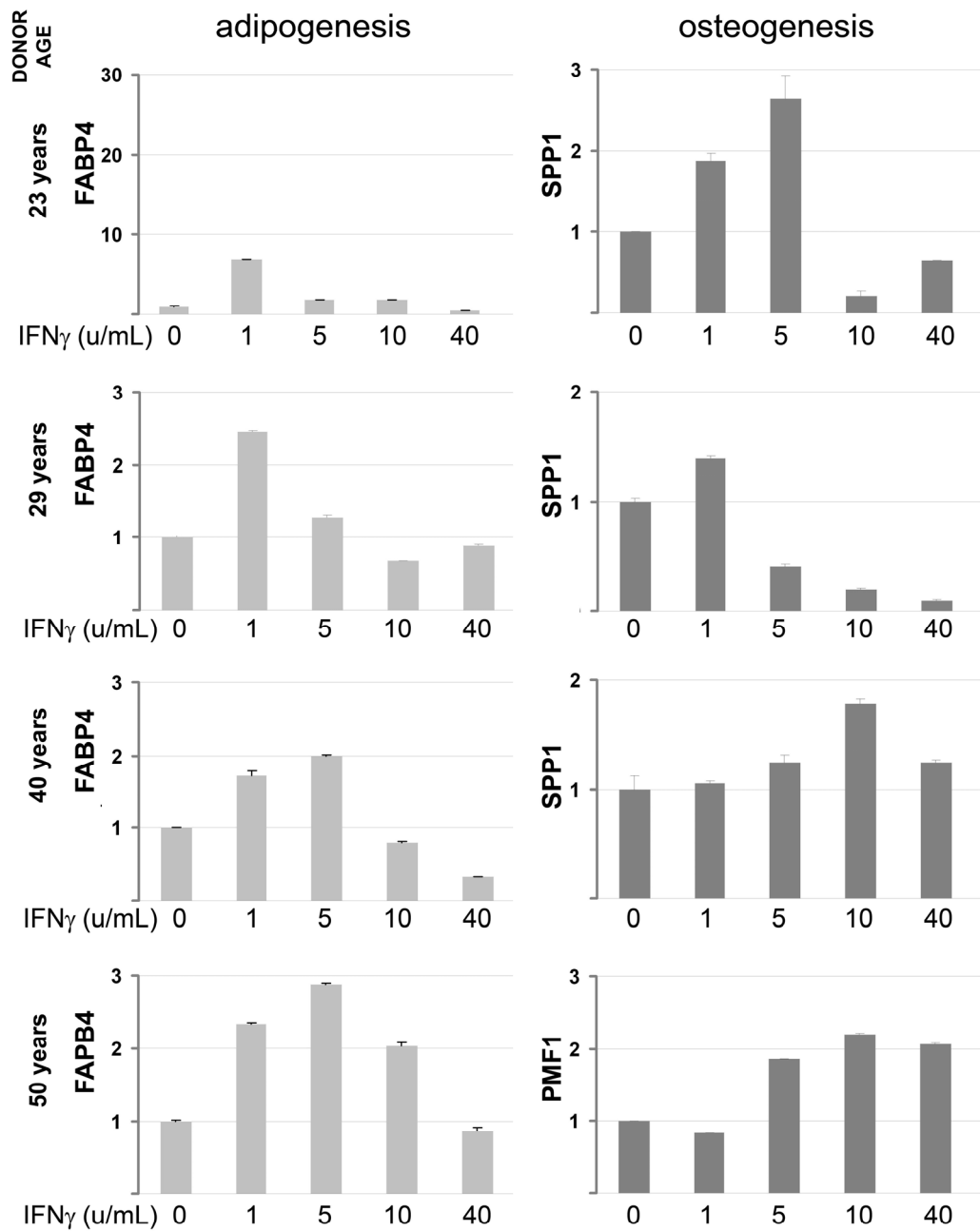


Figure 6

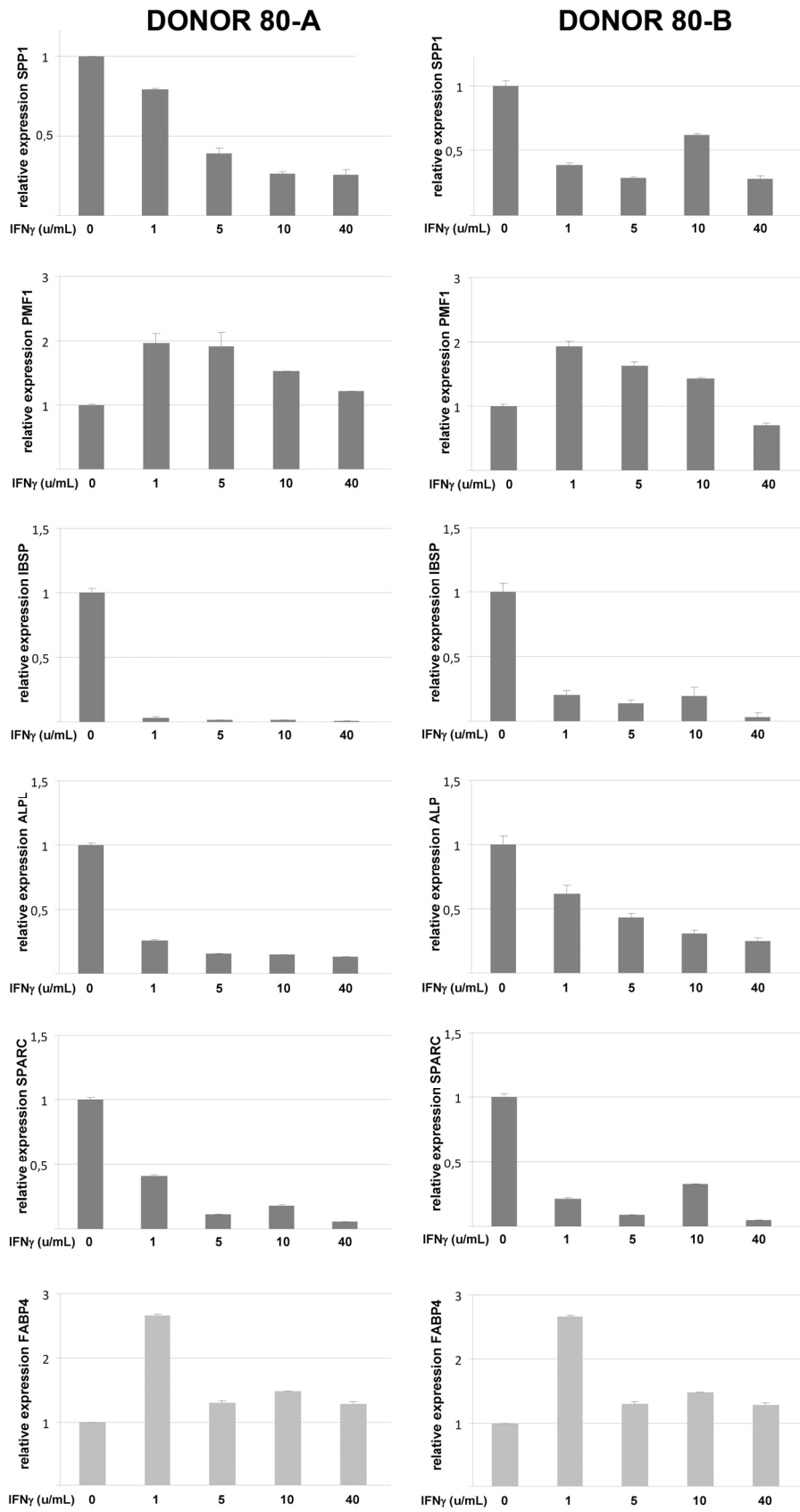
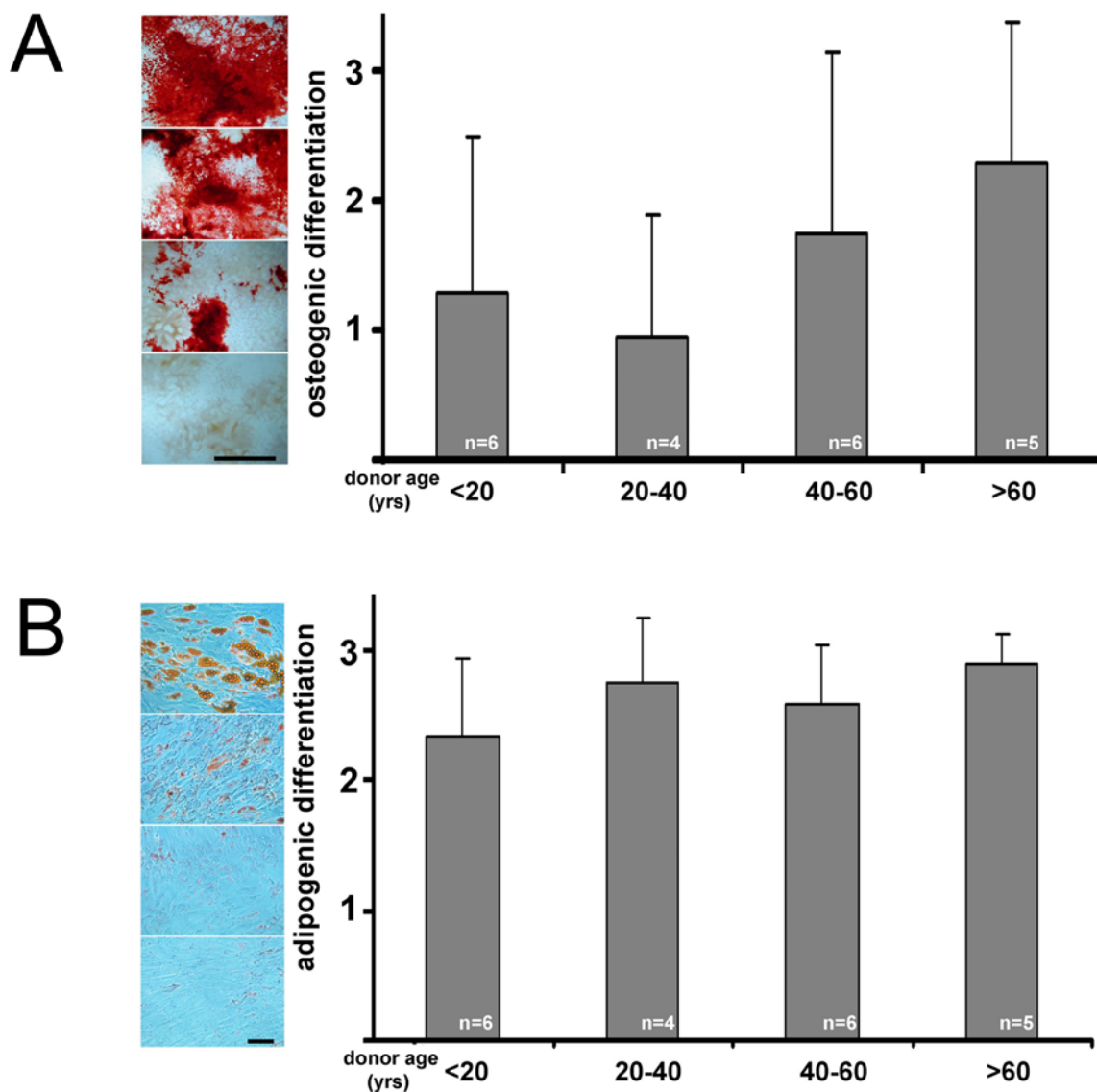


Figure 7

Supplementary Figure 1: Differentiation capacity of primary MSCs. (A)

Osteogenic and adipogenic differentiation *in vitro* (B). Differentiation capacity was determined in duplicates and staining was graded according to staining patterns as depicted at the left side of the respective panels; scale bar indicates 1cm (A) and 100 μm (B).



In vitro differentiation

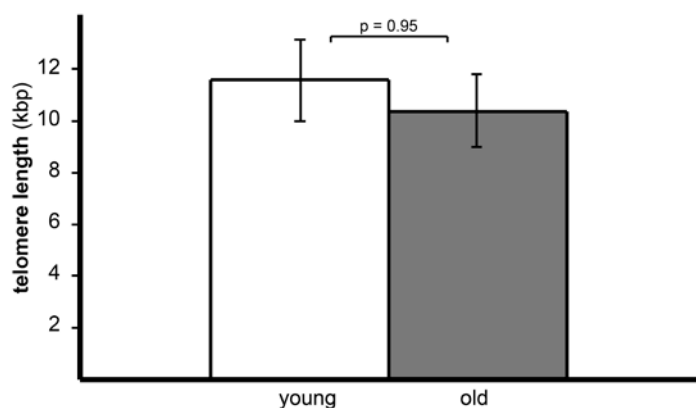
Differentiation was stimulated *in vitro* as described previously (Fehrer et al., 2007).

Briefly, MSC were plated in duplicates in 6-well plates at 50 cells/cm², grown to near confluence, and then induced to differentiate. In the case of primary cultures, 10⁵

total bone marrow cells/58cm² were grown for 7 - 10 days before induction. In any case, the induction medium was changed twice per week for a period of three weeks. Osteogenesis was stimulated using growth medium containing 1 mM β -glycerol phosphate, 100 nM dexamethasone, and 0.5 μ M ascorbate-2-phosphate. For evaluation, the cells were fixed with 4% *para*-formaldehyde / PBS for 10 minutes and stained with Alizarin Red, pH 4.1 for 20 minutes at ambient temperature. Excess stain was removed by several washes with PBS adjusted to pH 4. For adipogenic differentiation of MSC, growth medium was supplemented with 1 μ M dexamethasone, 60 μ M indomethacine, 0.5 mM 3-*iso*-butyl-1-methylxanthine, and 0.5 μ M hydrocortisone. After fixation, lipid vesicles in differentiated cells were stained with 0.7% Oil Red O in 85% propylene glycol for 20 minutes at room temperature. Excess stain was removed by several washes with PBS. The stained cells were scored with respect to their differentiation potential. For adipogenesis, undifferentiated cells were scored 0; small lipid vesicles around the nucleus, 1; small vesicles together with cells containing large lipid vacuoles, 2; predominantly large lipid vacuoles, 3. For osteogenesis, no differentiation was referred to as class 0; <40% positive cells, 1; 40-60%, 2; 60-100%, 3.

Fehrer, C., Brunauer, R., Laschober, G., Unterluggauer, H., Reitingner, S., Kloss, F., Gully, C., Gassner, R., and Lepperdinger, G. (2007). Reduced oxygen tension attenuates differentiation capacity of human mesenchymal stem cells and prolongs their lifespan. *Aging Cell* 6, 745-757.

Supplementary Figure 2 Mean telomere length of MSC derived from five young (9.1 +/- 2.9 years) and six elderly individuals (62.3 +/- 11.2 years).



DNA preparation and telomere length assessment

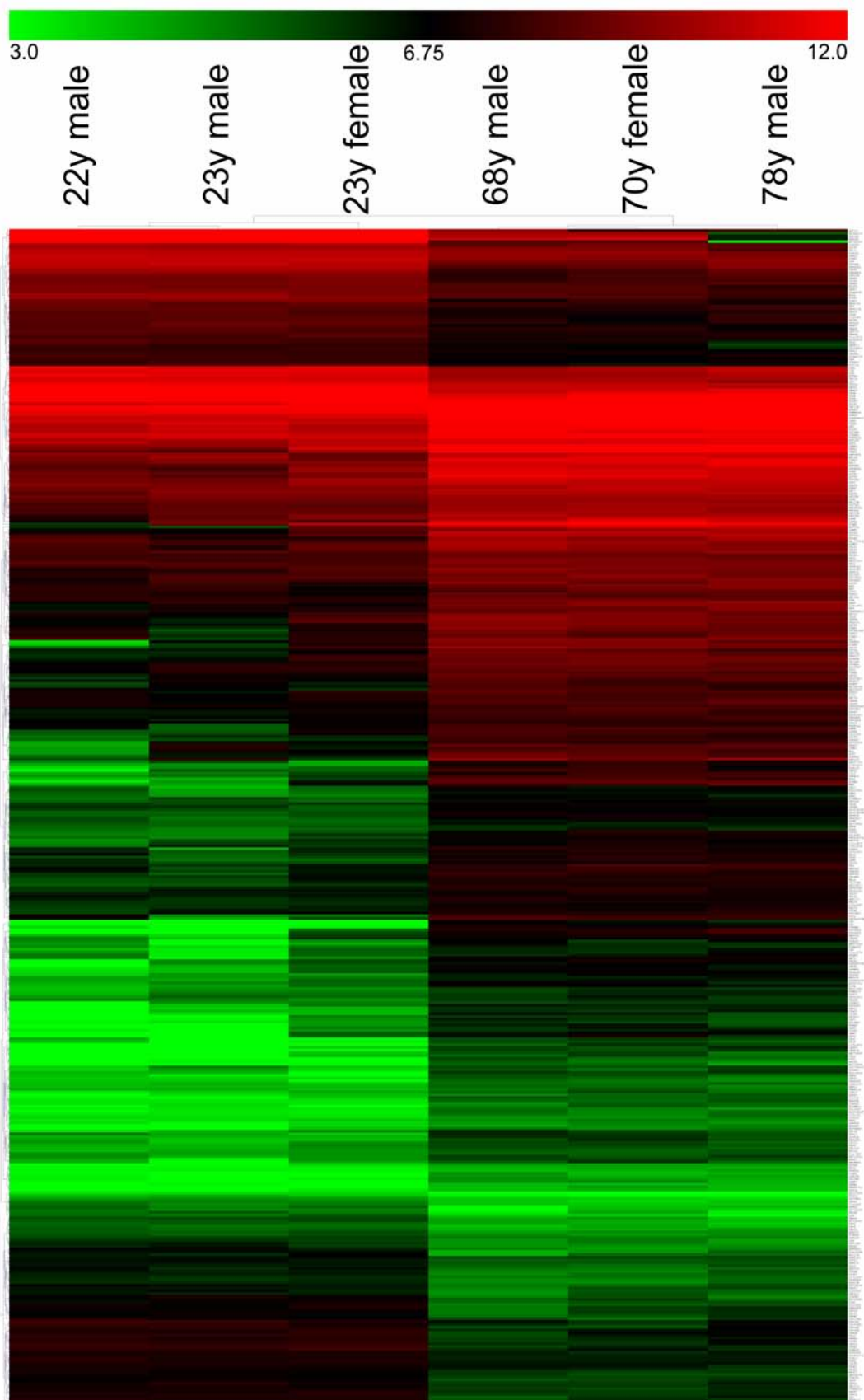
Telomere length was monitored by means of quantitative PCR essentially as designed by Cawthon (2002) following a modified protocol as described previously (Fehrer et al., 2006). As a standard for the telomere length assessment, human K562 leukaemia cells (ATTC number CCL-243) with short telomeres of 6.5 kbp, and TCL1301 with long telomeres of 27 kbp were employed. Prior to DNA isolation, cells were harvested and re-suspended in 100 mM Tris-HCl pH 8.5, 5 mM EDTA, 0.2% SDS, 200 mM NaCl, 100 µg/mL proteinaseK. The suspension was incubated at 55°C for 2 hours. Before phenol/chloroform/iso-amylalcohol (PCI) extraction, debris was removed by centrifugation at 10,000 x g. PCI extraction was repeated at least twice in order to yield a clear aqueous phase and interphase. Before alcohol precipitation, the solution was extracted once with chloroform/iso-amylalcohol. Large amounts of precipitated DNA were removed using a pipette tip, otherwise the precipitate was centrifuged and the pellet washed in 70% ethanol. The moist pellet was solved in 10 mM Tris-HCl pH 7.5, 1 mM EDTA by incubation over night at 55°C and the solution was stored at 4°C. In order to evaluate the telomeric repeat copies or T number of different DNA samples, the exact amount of genetic material coding for the single copy gene 36B4, or S number was used for calibration. Standard curves for telomere length and 36B4 amplification reactions were generated by plotting relative DNA concentration against C_t . The primers for the single copy gene 36B4 (acidic ribosomal phosphoprotein PO) which yield a 74 bp product, were 5' CAG CAA GTG GGA AGG TGT AAT CC 3' and 5' CCC ATT CTA TCA TCA ACG GGT ACA A 3'

(final concentration 0.3 μ M). The primer for the telomere PCR were 5' CGG TTT G (TTTGGG)₅ TT 3' and 5' GGC TTG CC(TTACCC)₅ T 3', each used at a final concentration of 0.2 μ M. PCR reactions with total DNA amount ranging from 180 ng to 247 pg, which yielded C_t values for S ranging from 20-25 were carried out using a Roche Light Cycler. Duplicate reactions with 5 μ L of each DNA dilution were performed in a 10 μ L volume using the Light Cycler Fast Start DNA Master SYBR Green I Kit (Roche), with MgCl₂ added to a final concentration of 3 mM. The PCR conditions were as follows: the enzyme was first activated for 10 minutes at 95°C. Next, the reaction for the single copy gene was 40 cycles at 95°C for 5 seconds, 58°C for 10 seconds and 72°C for 40 seconds, and for the telomeres 30 cycles at 95°C for 5 seconds, 56°C for 10 seconds and 72°C for 60 seconds, respectively. All transition rates were set to 20°C/second except the annealing temperature for the determination of telomere repeats was set to 4°C/second. After amplification of the single copy gene as well as of the telomeric repeat units, C_t values were plotted versus DNA concentration. Measurements were carried out in duplicates of three different DNA concentrations.

Cawthon, R.M. 2002. Telomere measurement by quantitative PCR. *Nucleic Acids Res* 30:e47.

Fehrer, C., Voglauer, R., Wieser, M., Pfister, G., Brunauer, R., Cioca, D., Grubeck-Loebenstein, B., and Lepperdinger, G. 2006. Techniques in gerontology: cell lines as standards for telomere length and telomerase activity assessment. *Exp Gerontol* 41:648-651.

Supplementary Figure 3: Hierarchical clustering of differentially expressed genes in primary mesenchymal stromal cells from three middle aged (22.7 +/- 0.6 years) and three elderly donors (72.0 +/- 5.3 years).

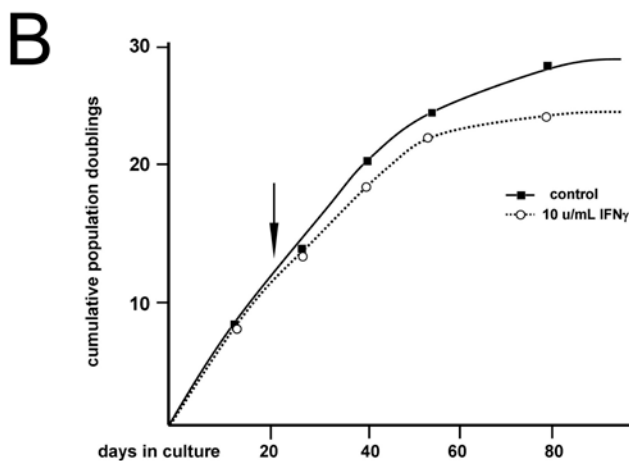
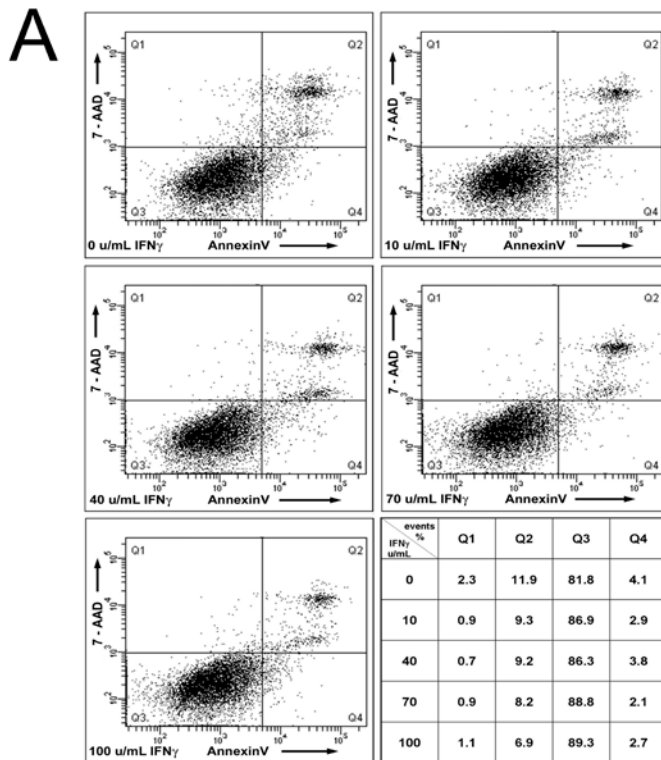


Whole genome expression analysis was performed using total RNA isolated from cultured mesenchymal stem cells. RNA was isolated from cultured mesenchymal stem cells after homogenization in 4.2 M guanidinium thiocyanate, phenol extraction and ethanol precipitation. Total mRNA was further processed for micro array analysis according to Affymetrix standardized procedures prior to hybridization onto Affymetrix Human Genome HU133 Plus 2.0 arrays. After normalization employing tools of the 'Comprehensive R based Microarray Analysis web frontend' CARMAweb1.5 (Rainer et al., 2006) 288 probe sets corresponding to 225 genes expressed at a higher level in the elderly group ($DE > 1.5$, $p < 0.05$, supplementary table 2), and 138 probe sets (118 genes) at a lower expression level were revealed (supplementary table 1). Hierarchical clustering (average linkage, Euclidean distance, samples and genes) was performed on all differentially expressed probe sets using Mev 4.5.0, part of the TM4 software suite, available online at <http://www.tm4.org/> (Saeed et al., 2006).

Rainer J, Sanchez-Cabo F, Stocker G, Sturn A, Trajanoski Z. CARMAweb: comprehensive R- and BioConductor-based web service for microarray data analysis. *Nucleic Acids Res.* 2006; 34:W498-W503

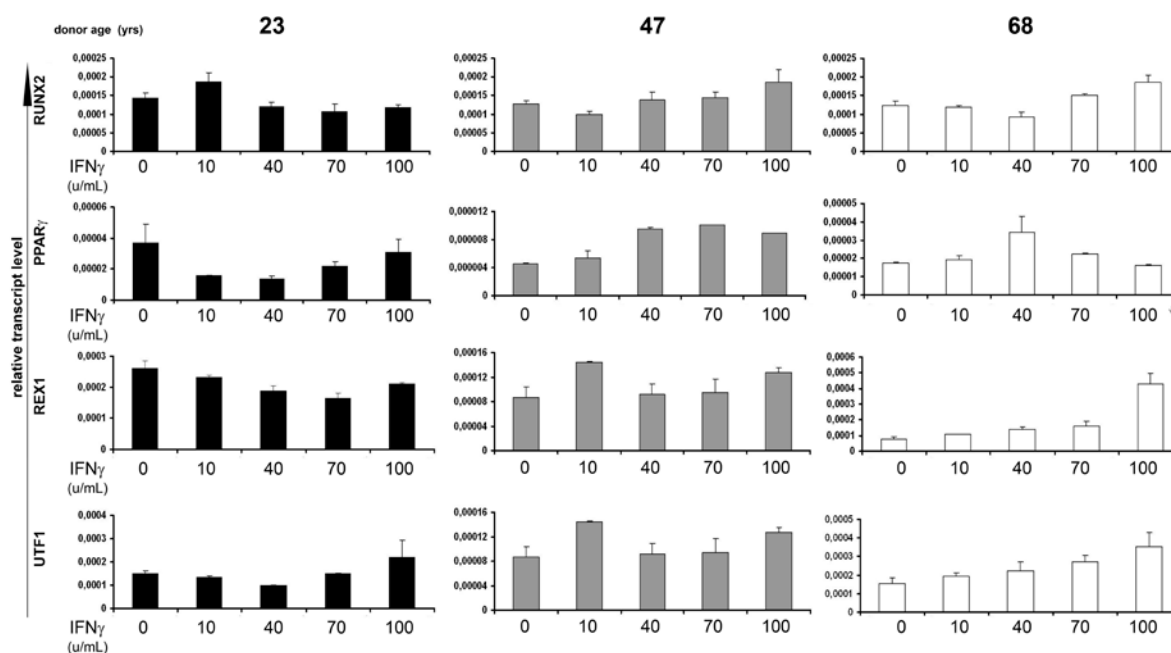
Saeed AI, Bhagabati NK, Braisted JC, Liang W, Sharov V, Howe EA, et al. TM4 microarray software suite . *Methods in Enzymology.* 2006;411:134-93.

Supplementary Figure 4: MSC at inflammatory stress. (A) flow cytometric assessment of cell death in cultured MSC after 24 hours of IFN γ treatment at indicated concentrations and quantitative evaluation (lower right); (B) proliferation of MSC in long-term culture in the continuous presence of 10 units/mL IFN γ , time point of addition of IFN γ is indicated by an arrow.



Supplementary Figure 5: Marker expression in MSC put at inflammatory stress.

Relative transcriptional activities of MSC at increasing concentration of IFN γ with respect to the stemness-associated transcription factors NANOG, REX1 and UTF1, as well as the osteogenic and adipogenic-specific transcription factors RUNX2 and PPAR γ as measured in triplicates by quantitative reverse transcription-PCR.



Quantitative Reverse Transcription-Polymerase Chain Reaction

RNA was isolated from cells after homogenization in 4.2 M guanidinium thiocyanate, phenol extraction and ethanol precipitation. cDNA was synthesized from total RNA using RevertAid H Minus-MMuLV-RT (Fermentas, St. Leon-Roth, Germany) and oligo(dT) primer (MWG, Germany). The assays were performed on a LightCycler 480 instrument (Roche, Austria) with the LC480-SYBR Green I Master kit (Roche, Austria). The 15 μ L reactions contained 2 μ M forward and reverse primer. After the activation of the enzyme at 95°C for 8 minutes, 50 cycles at 95°C for 15 seconds, 57°C for 8 seconds and 72°C for 15 seconds were performed. mRNA expression levels were calculated relative to eukaryotic translation elongation factor 1 alpha 1 (EEF1A1). Primer sequences and transcript IDs of the corresponding genes were as summarized as in Supplementary Table 3.

Supplementary Table 1: Primary MSC specification and donor information; primary colony-forming unit (pCFU), cumulative population doublings (CPD)

Donor #	Sex	age (years)	pCFU	CPD
1	m	5	140 +/- 16	65
2	f	6	228 +/- 0	53
3	m	7	88 +/- 8	31
4	m	10	160 +/- 19	48
5	m	10	202 +/- 23	49
6	m	10	124 +/- 6	58
7	m	11	141 +/- 9	n.d.
8	m	12	32 +/- 1	54
9	f	12	324 +/- 3	22
10	m	13	n.d.	55
11	f	13	130 +/- 0	n.d.
12	f	17	n.d.	22
13	m	22	235 +/- 39	24
14	m	22	22 +/- 8	22
15	m	23	203 +/- 21	24
16	f	23	197 +/- 7	30
17	m	33	151 +/- 6	41
18	f	40	126 +/- 3	37
19	f	45	131 +/- 13	n.d.
20	f	47	190 +/- 0	25
21	m	47	169 +/- 12	25
22	f	50	102 +/- 10	23
23	m	50	135 +/- 18	14
24	f	51	91 +/- 4	17
25	m	51	74 +/- 7	41
26	f	51	n.d.	n.d.
27	m	54	n.d.	45
28	f	56	165 +/- 48	27
29	m	63	133 +/- 25	21
30	f	65	84 +/- 13	29
31	m	68	84 +/- 2	16
32	f	70	n.d.	32
33	f	70	102 +/- 4	21
34	m	78	67 +/- 6	29

Supplementary Table 2: Whole genome expression analysis of primary mesenchymal stromal cells from three middle aged (22.7 +/- 0.6 years) and three elderly donors (72.0 +/- 5.3 years); list of differentially downregulated genes

GenBank ID	Description	Symbol	exp young ¹⁾	exp old ²⁾	DE ³⁾	p ⁴⁾
AI760252	---	---	5378.4	252.0	0.09	0.016
AU144114	---	---	9808.6	740.6	0.12	<0.001
U43328	hyaluronan & proteoglycan link protein 1	HAPLN1	11189.6	1457.0	0.21	0.003
NM_005159	actin, alpha, cardiac muscle 1	ACTC1	5028.1	500.2	0.22	0.002
NM_001884	hyaluronan and proteoglycan link protein 1	HAPLN1	8339.7	905.5	0.22	0.046
NM_002204	integrin, alpha 3 (antigen CD49C, alpha 3 subunit of VLA-3 receptor)	ITGA3	238.9	65.4	0.32	0.001
M79321	v-yes-1 Yamaguchi sarcoma viral related oncogene homolog	LYN	165.7	39.9	0.39	0.008
AI127800	scavenger rec. class F, member 2	SCARF2	133.9	34.0	0.40	0.006
AA458879	ankyrin repeat domain 52	ANKRD52	94.8	26.9	0.41	0.024
NM_002350	v-yes-1 Yamaguchi sarcoma viral related oncogene homolog	LYN	36.7	10.1	0.42	0.006
BG334196	EH domain binding protein 1-like 1	EHBP1L1	170.0	58.3	0.42	0.002
NM_016458	Chromos 8 open reading frame 30A	C8orf30A	96.5	26.6	0.42	0.007
Z54367	plectin 1, intermediate filament binding protein 500kDa	PLEC1	657.9	170.9	0.45	0.003
BE783949	Chromos. 9 open reading frame 86	C9orf86	138.3	38.9	0.45	0.022
NM_024031	proline rich 14	PRR14	170.6	61.9	0.46	<0.001
NM_024958	neurensin 2	NRSN2	70.3	24.4	0.46	0.031
U83867	spectrin, alpha, non-erythrocytic 1 (alpha-fodrin)	SPTAN1	1732.8	547.7	0.47	0.019
NM_017980	LIM and senescent cell antigen-like domains 2	LIMS2	166.1	46.2	0.47	0.006
NM_000445	plectin 1, intermediate filament binding protein 500kDa	PLEC1	430.7	135.1	0.47	0.024
U36190	cysteine-rich protein 2	CRIP2	1195.0	363.9	0.48	0.001
BF941088	coiled-coil domain containing 50	CCDC50	1321.9	431.5	0.48	0.003
NM_016104	RWD domain containing 1	RWDD1	4219.9	1724.5	0.49	0.005
NM_014766	secernin 1	SCRN1	1005.7	335.8	0.49	0.008
U48734	actinin, alpha 4	ACTN4	3108.9	1124.5	0.49	0.007

NM_022089	ATPase type 13A2	ATP13A2	73.7	25.2	0.49	0.012
BC016767	---	---	46.2	18.2	0.50	0.007
NM_004082	dynactin 1 (p150, glued homolog, Drosophila)	DCTN1	611.8	261.0	0.50	0.003
AF256215	aryl hydrocarbon receptor nuclear translocator-like 2	ARNTL2	229.9	87.5	0.51	0.009
AL137520	F-box protein 9	FBXO9	50.0	18.7	0.51	0.001
AB047005	microtubule associated serine/threonine kinase 2	MAST2	136.3	59.5	0.51	0.019
U29725	mitogen-activated protein kinase 7	MAPK7	153.1	65.4	0.51	<0.001
AF323728	oxysterol binding protein-like 6	OSBPL6	223.6	78.2	0.52	0.014
AF222711	C-terminal binding protein 2	CTBP2	1925.1	844.7	0.52	<0.001
BC002323	zyxin	ZYX	1823.5	709.7	0.52	0.009
AA161130	proline rich 14	PRR14	215.7	78.1	0.52	0.001
NM_003461	zyxin	ZYX	2753.4	1184.2	0.52	0.003
AI689676	zinc finger protein 579	ZNF579	87.6	44.5	0.53	<0.001
AF274938	retinitis pigmentosa 9 pseudogene	LOC441212	166.7	78.9	0.53	0.008
NM_031283	transcription factor 7-like 1 (T-cell specific, HMG-box)	TCF7L1	300.5	102.3	0.54	0.035
AA531086	tropomyosin 2 (beta)	TPM2	39.3	17.3	0.54	0.002
AI912275	B-cell CLL/lymphoma 11A (zinc finger protein)	BCL11A	87.1	29.7	0.54	0.028
N45308	diacylglycerol kinase, theta 110kDa	DGKQ	168.8	81.1	0.54	0.008
NM_015540	RNA polymerase II assoc. protein 1	RPAP1	28.4	13.5	0.55	<0.001
AI286226	thyroid adenoma associated	THADA	356.0	170.2	0.55	<0.001
NM_005167	protein phosphatase 1J (PP2C domain containing)	PPM1J	6326.3	2328.3	0.55	0.003
NM_017859	uridine-cytidine kinase 1-like 1	UCKL1	162.0	78.3	0.55	0.011
D64109	transducer of ERBB2, 2	TOB2	118.3	44.8	0.55	0.024
BC002669	nuclear receptor subfamily 2, group F, member 6	NR2F6	382.4	174.7	0.56	0.016
BF515750	chromosome 1 open reading frame 131	C1orf131	316.5	153.0	0.56	0.028
AW051856	filamin A, alpha (actin binding protein 280)	FLNA	10916.9	4543.3	0.56	0.017
AB011174	phosphofurin acidic cluster sorting protein 2	PACS2	124.5	50.6	0.56	0.008
AC005600	tuberous sclerosis 2	TSC2	214.0	84.4	0.56	0.024
NM_014652	importin 13	IPO13	92.0	44.4	0.56	0.002

NM_007219	ring finger protein 24	RNF24	361.5	151.4	0.57	0.016
NM_002807	proteasome (prosome, macropain) 26S subunit, non-ATPase, 1	PSMD1	1666.1	736.5	0.57	0.005
BC004419	vacuolar protein sorting 24 homolog (<i>S. cerevisiae</i>)	VPS24	2278.2	1211.9	0.57	<0.001
NM_004309	Rho GDP dissociation inhibitor (GDI) alpha	ARHGDI A	919.7	307.6	0.57	0.004
Z67743	chloride channel 7	CLCN7	164.5	88.8	0.57	0.001
AI467916	AXL receptor tyrosine kinase	AXL	160.4	62.6	0.57	0.004
NM_018275	chromosome 7 open reading frame 43	C7orf43	29.5	13.8	0.57	0.017
NM_002097	general transcription factor IIIA	GTF3A	3472.5	1780.3	0.58	0.011
AB002321	KIAA0323	KIAA0323	136.6	61.3	0.58	0.006
AL353715	stathmin-like 3	STMN3	182.1	71.3	0.58	0.009
BG285881	prickle homolog 2 (<i>Drosophila</i>)	PRICKLE2	120.0	44.3	0.58	0.006
AK000722	solute carrier family 27 (fatty acid transporter), member 4	SLC27A4	126.3	48.6	0.58	0.021
BE379542	chromodomain helicase DNA binding protein 3	CHD3	119.8	54.6	0.58	0.001
AB030034	sterile alpha motif and leucine zipper containing kinase AZK	ZAK	245.4	116.3	0.58	0.004
AK024446	ATP-binding cassette, sub-family C (CFTR/MRP), member 10	ABCC10	137.6	64.7	0.58	0.009
AI744229	CDGSH iron sulfur domain 3	CISD3	82.9	34.9	0.58	0.009
H28667	sterile alpha motif and leucine zipper containing kinase AZK	ZAK	2789.7	1150.4	0.58	0.005
NM_017949	CUE domain containing 1	CUEDC1	119.0	56.0	0.59	0.009
AI143307	zinc finger protein 598	ZNF598	88.1	34.9	0.59	0.049
BC006230	monoglyceride lipase	MGLL	847.2	302.6	0.59	0.025
AI356412	v-yes-1 Yamaguchi sarcoma viral related oncogene homolog	LYN	61.4	25.4	0.59	0.003
AF037261	sorbin and SH3 domain containing 3	SORBS3	242.1	117.2	0.59	0.009
AW593303	ATPase family, AAA domain containing 3B	ATAD3B	70.2	30.5	0.59	0.004
AF312028	protein phosphatase 1, regulatory (inhibitor) subunit 12C	PPP1R12C	102.1	38.7	0.60	0.027
AB018345	KIAA0802	KIAA0802	690.9	318.6	0.60	0.020
AI916284	---	---	30.6	12.3	0.60	0.013
NM_153358	zinc finger protein 791	ZNF791	365.9	162.5	0.60	0.015
NM_001456	filamin A, alpha (actin binding protein 280)	FLNA	8691.2	4018.1	0.60	0.016
U50383	SMYD family member 5	SMYD5	37.1	13.5	0.60	0.010

AI937468	chromosome 12 open reading frame 52	C12orf52	70.2	35.8	0.60	<0.001
NM_024319	chromosome 1 open reading frame 35	C1orf35	88.2	35.8	0.60	0.020
AA844682	synovial apoptosis inhibitor 1, synoviolin	SYVN1	186.7	75.2	0.60	0.009
BC005851	Rho GDP dissociation inhibitor (GDI) alpha	ARHGDI A	1477.5	551.1	0.61	0.014
AK026954	retinoblastoma binding protein 6	RBBP6	348.8	174.8	0.61	0.006
AL037626	---	---	11.1	6.2	0.61	<0.001
NM_001687	ATP synthase, H ⁺ transporting, mitochondrial F1 complex, delta subunit	ATP5D	123.6	53.6	0.61	0.015
AW664056	---	---	122.6	53.4	0.61	0.003
AW449169	speckle-type POZ protein	SPOP	36.5	16.9	0.62	0.003
AI494567	suppressor of Ty 6 homolog (<i>S. cerevisiae</i>)	SUPT6H	175.5	86.1	0.62	0.003
NM_001345	diacylglycerol kinase, alpha 80kDa	DGKA	366.5	168.7	0.62	0.003
BE963280	sterile alpha motif domain containing 4B	SAMD4B	54.2	31.0	0.62	0.010
NM_003942	ribosomal protein S6 kinase, 90kDa, polypeptide 4	RPS6KA4	68.3	30.4	0.62	0.002
NM_016453	NCK interacting protein with SH3 domain	NCKIPSD	150.1	80.7	0.62	0.009
NM_006715	mannosidase, alpha, class 2C, member 1	MAN2C1	44.2	23.8	0.63	0.007
BF515124	FRY-like	FRYL	321.8	129.4	0.63	0.015
BC004820	chromos 13 open reading frame 8	C13orf8	390.5	168.1	0.63	0.015
BC000850	F-box and WD repeat domain containing 5	FBXW5	117.3	50.2	0.63	0.017
BC002799	SAPS domain family, member 1	SAPS1	154.4	66.8	0.63	0.034
NM_013403	striatin, calmodulin binding protein 4	STRN4	82.4	34.5	0.63	0.006
NM_030971	sideroflexin 3	SFXN3	582.9	269.5	0.63	0.004
AA149545	EH domain binding protein 1-like 1	EHBP1L1	94.2	52.5	0.63	0.022
U36501	SP100 nuclear antigen	SP100	133.7	69.1	0.63	0.002
BE620258	Fanconi anemia, complementation group L	FANCL	15.2	8.3	0.64	0.009
AL137394	TEL2, telomere maintenance 2, homolog (<i>S. cerevisiae</i>)	TELO2	39.9	19.0	0.64	0.004
AI493119	zinc finger protein 512B	ZNF512B	444.8	197.9	0.64	0.004
AI625550	filamin A, alpha (actin binding protein 280)	FLNA	5465.4	2495.9	0.64	0.029
AF039693	serologically defined colon cancer antigen 10	SDCCAG10	232.9	102.8	0.64	0.006
NM_007061	CDC42 effector protein (Rho GTPase binding) 1	CDC42EP1	192.2	76.1	0.64	0.026

AI885670	selenophosphate synthetase 1	SEPHS1	237.8	134.1	0.64	0.017
AI798908	KIAA0226	KIAA0226	243.6	124.5	0.64	0.002
AI697751	Wolf-Hirschhorn syndrome candidate 1-like 1	WHSC1L1	471.7	200.7	0.64	0.018
NM_004581	Rab geranylgeranyltransferase, alpha subunit	RABGGTA	134.6	54.5	0.64	0.017
NM_002743	protein kinase C substrate 80K-H	PRKCSH	674.8	295.5	0.64	0.012
AI492167	retinitis pigmentosa 9 (autosomal dominant)	RP9	445.4	234.5	0.64	0.008
BG547855	pleiomorphic adenoma gene-like 1	PLAGL1	1612.1	856.9	0.64	0.014
AI745624	elongation factor, RNA polymerase II, 2	ELL2	1452.7	624.6	0.65	0.022
AF309082	protein kinase D2	PRKD2	83.9	43.1	0.65	0.028
NM_021131	protein phosphatase 2A activator, regulatory subunit 4	PPP2R4	239.3	94.3	0.65	0.018
AA744771	zinc finger protein 22 (KOX 15)	ZNF22	623.4	313.7	0.65	0.017
AI817830	MYST histone acetyltransferase (monocytic leukemia) 3	MYST3	614.1	299.9	0.65	0.008
NM_000436	3-oxoacid CoA transferase 1	OXCT1	1034.0	534.8	0.65	0.011
T84558	NIPA-like domain containing 3	NPAL3	231.9	132.6	0.65	0.011
NM_001977	glutamyl aminopeptidase (aminopeptidase A)	ENPEP	36.8	13.0	0.66	0.018
NM_004517	integrin-linked kinase	ILK	2934.1	1464.4	0.66	0.019
AA682499	kinesin light chain 3	KLC3	82.5	42.1	0.66	0.004
NM_014664	Nedd4 binding protein 1	N4BP1	147.0	83.0	0.66	0.010
NM_006702	patatin-like phospholipase domain containing 6	PNPLA6	203.2	67.3	0.66	0.011
NM_003443	zinc finger and BTB domain containing 17	ZBTB17	79.3	35.8	0.66	0.013
BE646638	FCH and double SH3 domains 1	FCHSD1	44.9	24.3	0.66	0.008
BF060782	tumor protein p53 binding protein 1	TP53BP1	21.8	12.7	0.66	0.002
NM_030817	apolipoprotein L domain containing 1	APOLD1	417.8	175.4	0.66	0.013
AI655015	---	---	290.5	151.4	0.66	0.030
NM_003334	ubiquitin-activating enzyme E1	UBE1	2905.9	1103.0	0.66	0.014
NM_022065	thyroid adenoma associated	THADA	173.5	84.5	0.66	0.017
M95929	sideroflexin 3	SFXN3	625.7	337.5	0.67	0.002

1 average expression level in young age group; 2 average expression level in old age group; 3 differential expression; 4 p-value was calculated using Student's T-test (two-tailed, two-sample, unequal variance)

Supplementary Table 3: Whole genome expression analysis of primary mesenchymal stromal cells from three middle aged (22.7 +/- 0.6 years) and three elderly donors (72.0 +/- 5.3 years); list of differentially upregulated genes

GenBank ID	Description	Symbol	exp young ¹⁾	exp old ²⁾	DE ³⁾	p ⁴⁾
NM_000204	complement factor I	CFI	3.9	87.8	15.88	0.023
BC020718	complement factor I	CFI	7.5	113.5	11.44	0.013
AB062292	catenin (cadherin-associated protein), beta 1, 88kDa	CTNNB1	8.5	131.0	8.42	0.012
BC035749	chromos 13 open reading frame 31	C13orf31	5.4	52.1	6.92	0.032
NM_153218	chromosome 13 open reading frame 31	C13orf31	20.3	181.5	6.58	0.022
AL711520	small EDRK-rich factor 1A (telomeric)	SERF1A	7.1	54.2	5.52	0.008
U78577	phosphatidylinositol-4-phosphate 5-kinase, type I, alpha	PIP5K1A	16.0	210.5	5.24	0.021
AI811298	odd-skipped related 2 (Drosophila)	OSR2	6.7	42.1	4.82	0.027
NM_080671	potassium voltage-gated channel, Isk-related family, member 4	KCNE4	39.5	425.3	4.54	<0.001
BU175810	ARP2 actin-related protein 2 homolog (yeast)	ACTR2	186.4	1526.7	4.07	0.008
AI659800	chromosome 13 open reading frame 31	C13orf31	123.2	686.8	4.06	0.006
NM_001415	eukaryotic translation initiation factor 2, subunit 3 gamma, 52kDa	EIF2S3	167.6	1901.3	4.06	0.004
AB033281	F-box and WD repeat domain containing 11	FBXW11	39.4	266.5	4.02	<0.001
AF147437	exostoses (multiple) 1	EXT1	21.2	130.9	3.97	<0.001
NM_006815	transmembrane emp24 domain trafficking protein 2	TMED2	632.4	4991.6	3.93	<0.001
AU151239	transmembrane and tetra-tricopeptide repeat containing 1	TMTC1	12.1	71.3	3.86	<0.001
BC036253	ARP2 actin-related protein 2 homolog (yeast)	ACTR2	467.3	2968.3	3.84	0.023
NM_015962	FCF1 small subunit (SSU) processome component homolog (S. cerevisiae)	FCF1	29.4	308.4	3.69	0.026
AFFX-R2-BS-DAP-5		---	678.0	7718.8	3.68	0.046
AI343000	sorbin & SH3 domain containing 2	SORBS2	65.4	424.9	3.64	0.031
NM_002290	laminin, alpha 4	LAMA4	340.3	2709.9	3.62	0.040
NM_080671	potassium voltage-gated channel, Isk-related family, member 4	KCNE4	73.9	581.5	3.60	0.003
BF576710	protein tyrosine phosphatase type IVA, member 1	PTP4A1	278.5	1522.0	3.57	0.001
NM_005419	signal transducer and activator of transcription 2, 113kDa	STAT2	12.9	71.1	3.56	0.010

NM_001228	caspase 8, apoptosis-related cysteine peptidase	CASP8	9.4	59.7	3.50	0.021
BC035329	sorbin & SH3 domain containing 2	SORBS2	51.6	252.2	3.47	<0.001
BC005379	plasminogen-like B2	PLGLB2	19.1	98.3	3.46	0.008
AI022387	heterogeneous nuclear ribonucleoprotein H1 (H)	HNRPH1	10.3	41.0	3.46	0.008
AW338933	TIMP metallopeptidase inhibitor 3 (Sorsby fundus dystrophy, pseudoinflammatory)	TIMP3	628.2	3400.5	3.39	0.007
AFFX-R2-BS-DAP-M		---	1637.0	12867.3	3.27	0.048
AA699583	ARP2 actin-related protein 2 homolog (yeast)	ACTR2	544.6	2616.2	3.25	0.024
AFFX-DAPX-M		---	1276.0	10402.1	3.23	0.040
AF308601	Notch homolog 2 (Drosophila)	NOTCH2	453.9	2447.7	3.21	0.027
NM_144664	family with sequence similarity 76, member B	FAM76B	85.5	499.8	3.16	0.033
NM_006815	transmembrane emp24 domain trafficking protein 2	TMED2	1193.5	7559.4	3.14	0.001
R11654	dimethylarginine dimethylaminohydrolase 1	DDAH1	121.2	647.3	3.07	0.044
BF109231	transmembrane and tetra-tricopeptide repeat containing 1	TMTC1	29.9	221.8	3.05	0.050
U67195	TIMP metallopeptidase inhibitor 3 (Sorsby fundus dystrophy, pseudoinflammatory)	TIMP3	1076.0	4771.4	3.00	<0.001
AW006750	kelch-like 24 (Drosophila)	KLHL24	24.9	187.3	2.99	0.049
AB047847	coatamer protein complex, subunit gamma 2	COPG2	34.0	167.0	2.97	0.021
AFFX-R2-BS-DAP-3		---	3577.8	16889.8	2.97	0.035
NM_020351	collagen, type VIII, alpha 1	COL8A1	10.1	43.1	2.96	<0.001
NM_014456	programmed cell death 4 (neo-plastic transformation inhibitor)	PDCD4	120.0	634.7	2.91	0.026
BF677084	---	---	15.1	81.7	2.89	0.049
AFFX-DAPX-3		---	2393.4	12727.5	2.89	0.042
BC010956	fibroblast growth factor 7 (keratinocyte growth factor)	FGF7	73.4	412.0	2.85	0.022
BC036005	vacuolar protein sorting 8 homolog (S. cerevisiae)	VPS8	9.7	46.5	2.83	0.001
U35004	mitogen-activated protein kinase 8	MAPK8	7.2	32.8	2.83	0.032
AA723514	MYC associated factor X	MAX	134.1	617.7	2.83	0.042
BC038209	integrin, beta 8	ITGB8	10.7	73.8	2.81	0.049
AK024248	hypothetical gene supported by AK024248; AL137733	FLJ14186	14.2	58.7	2.80	0.002

U78576	phosphatidylinositol-4-phosphate 5-kinase, type I, alpha	PIP5K1A	21.5	207.0	2.80	0.044
S69738	chemokine (C-C motif) ligand 2	CCL2	33.3	237.0	2.79	0.045
BF347089	TIMP metalloproteinase inhibitor 3 (Sorsby fundus dystrophy, pseudoinflammatory)	TIMP3	2115.5	7547.9	2.73	<0.001
NM_006432	Niemann-Pick disease, type C2	NPC2	691.5	2846.1	2.73	0.013
BG484314	syntrophin, beta 1 (dystrophin-associated protein A1, 59kDa, basic component 1)	SNTB1	118.8	436.3	2.64	0.008
NM_003522	histone cluster 1, H2bf	HIST1H2BF	9.4	32.9	2.62	0.015
BG532405	chromosome 13 open reading frame 1	C13orf1	10.2	32.6	2.61	0.018
AI084086	golgi SNAP receptor complex member 2	GOSR2	13.7	75.1	2.60	0.003
AA495775	purine-rich element binding protein B	PURB	24.4	113.1	2.56	0.005
BC002649	histone cluster 1, H1c	HIST1H1C	93.9	353.9	2.56	0.002
M83248	secreted phosphoprotein 1 (osteopontin, bone sialoprotein I, early T-lymphocyte activation 1)	SPP1	10.5	53.2	2.54	0.002
AF116671			50.1	176.5	2.51	0.002
AB018580	aldo-keto reductase family 1, member C3 (3-alpha hydroxy-steroid dehydrogenase, type II)	AKR1C3	104.2	789.1	2.49	0.027
AW974077	activin A receptor, type IIA	ACVR2A	17.7	59.0	2.48	0.029
M64240	MYC associated factor X	MAX	49.7	372.0	2.45	0.048
AL110298	solute carrier family 2 (facilitated glucose transporter), member 3	SLC2A3	128.4	534.2	2.43	0.001
U10473	UDP-Gal:betaGlcNAc beta 1,4- galactosyltransferase, polypept. 1	B4GALT1	24.0	117.7	2.43	0.006
AI652192	Mitoch. ribosomal protein S28	MRPS28	24.7	81.5	2.43	0.004
NM_030804	frizzled homolog 5 (Drosophila)	FZD5	47.7	175.6	2.42	0.039
AK021715	---	---	32.6	184.9	2.41	0.038
NM_004343	calreticulin	CALR	166.5	744.0	2.41	0.022
AI733194	---	---	5.8	31.5	2.39	0.048
AF294326	core-binding factor, beta subunit	CBFB	88.7	320.4	2.38	0.002
AB046841	protocadherin beta 16	PCDHB16	9.1	34.9	2.36	0.024
NM_003523	histone cluster 1, H2be	HIST1H2BE	40.7	126.0	2.36	0.022
M22921	UDP-Gal:betaGlcNAc beta 1,4- galactosyltransferase, polypept. 1	B4GALT1	17.3	80.9	2.35	0.009
AC003007	hypothetical protein LOC440345	LOC440345	120.9	502.6	2.34	0.008

NM_001078	vascular cell adhesion molecule 1	VCAM1	684.8	4555.3	2.34	0.035
NM_002130	3-hydroxy-3-methylglutaryl-Coenzyme A synthase 1 (soluble)	HMGCS1	27.6	142.0	2.34	0.006
M18468	protein kinase, cAMP-dependent, regulatory, type I, alpha (tissue specific extinguisher 1)	PRKAR1A	518.1	2357.2	2.33	0.003
BF061543	pregnancy-associated plasma protein A, pappalysin 1	PAPPA	59.1	216.5	2.30	0.024
BF057492	TRK-fused gene	TFG	73.9	255.4	2.28	0.026
AK025101	exostoses (multiple) 1	EXT1	189.4	777.6	2.28	0.016
NM_004877	glia maturation factor, gamma	GMFG	11.1	43.2	2.26	0.007
AF237813	4-aminobutyrate aminotransferase	ABAT	172.7	794.8	2.25	0.047
AL137266	Williams Beuren syndrome chromosome region 19	WBSCR19	17.0	55.8	2.24	0.026
NM_003945	ATPase, H ⁺ transporting, lysosomal 9kDa, V0 subunit e1	ATP6V0E1	393.7	1042.4	2.24	0.001
NM_024560	FLJ21963 protein	FLJ21963	21.2	59.0	2.23	0.001
AW274468	---	---	8.9	44.5	2.23	0.031
H72914	sorbin & SH3 domain containing 2	SORBS2	10.6	34.7	2.22	0.047
NM_001839	calponin 3, acidic	CNN3	1942.3	5947.6	2.21	0.023
BC001364	SEC22 vesicle trafficking protein homolog B (<i>S. cerevisiae</i>)	SEC22B	429.1	1226.5	2.21	0.003
AI378788	discoidin, CUB and LCCL domain containing 2	DCBLD2	19.1	89.7	2.20	0.030
AA521381	solute carrier family 30 (zinc transporter), member 7	SLC30A7	9.9	29.4	2.19	0.034
NM_145297	zinc finger protein 626	ZNF626	44.0	132.0	2.18	0.014
AB030710	GABA(A) receptor-associated protein-like 2	GABARAPL2	1906.1	5262.7	2.18	0.001
AW957786	sprouty-related, EVH1 domain containing 1	SPRED1	22.0	110.8	2.18	0.006
NM_002586	pre-B-cell leukemia homeobox 2	PBX2	31.3	90.7	2.18	0.006
D25284	galactosylceramidase	GALC	9.2	42.8	2.18	0.024
AW043713	sulfatase 1	SULF1	3046.9	12130.9	2.17	0.003
AA284256	meningioma expressed antigen 5 (hyaluronidase)	MGEA5	10.5	73.4	2.16	0.032
AA569225	lipoma HMGIC fusion partner	LHFP	48.7	174.1	2.16	0.005
AF161422	hypothetical protein DKFZp564O0523	DKFZP564O0523	26.3	85.9	2.12	0.004
BF125756	GABA(A) receptor-associated protein like 1	GABARAPL1	141.4	497.3	2.12	0.031

AF356518	junctional adhesion molecule 3	JAM3	17.4	111.8	2.12	0.006
NM_173594	---	---	318.0	1027.7	2.11	0.002
NM_004878	prostaglandin E synthase	PTGES	213.5	975.1	2.10	0.036
AF358829	mediator complex subunit 28	MED28	65.8	165.1	2.10	0.012
BF127479	ribonuclease H1	RNASEH1	103.5	268.3	2.10	0.007
AI631159	solute carrier family 2 (facilitated glucose transporter), member 3	SLC2A3	375.7	1090.6	2.09	0.011
NM_021021	syntrophin, beta 1 (dystrophin-associated protein A1, 59kDa, basic component 1)	SNTB1	21.6	95.2	2.07	0.004
BE669703	---	---	6.1	17.9	2.05	0.019
AF021233	tumor necrosis factor receptor superfamily, member 10d, decoy with truncated death domain	TNFRSF10D	36.9	126.2	2.05	0.019
AI680874	hypothetical protein FLJ23861	FLJ23861	35.8	106.8	2.04	0.003
AV700591	phosphodiesterase 4D interacting protein (myomegalin)	PDE4DIP	22.4	72.2	2.03	0.004
S81916	phosphoglycerate kinase 1	PGK1	173.1	481.4	2.03	0.003
AU146493	development and differentiation enhancing factor 1	DDEF1	6.9	22.6	2.02	0.021
AI700633	serine incorporator 5	SERINC5	695.2	1926.8	2.02	0.003
BC001441	S-phase kinase-associated protein 2 (p45)	SKP2	32.4	108.7	2.02	0.020
AU145225	caldesmon 1	CALD1	122.7	812.5	2.01	0.034
NM_018375	solute carrier family 39 (zinc transporter), member 9	SLC39A9	56.4	160.4	2.00	0.003
BF439983	caspase 8, apoptosis-related cysteine peptidase	CASP8	124.9	368.2	2.00	0.013
BE672140	SFRS protein kinase 2	SRPK2	12.6	36.5	1.98	0.043
BG427809	BMS1 pseudogene 5	BMS1P5	78.4	229.6	1.98	0.003
BF697247	sterile alpha motif domain cont. 4A	SAMD4A	10.3	24.5	1.96	0.007
AI753143	integrin, beta-like 1 (with EGF-like repeat domains)	ITGBL1	156.3	509.1	1.96	0.032
AK025665	patatin-like phospholipase domain containing 3	PNPLA3	40.4	112.3	1.96	0.024
AW847318	mastermind-like 2 (Drosophila)	MAML2	18.1	53.5	1.96	0.008
AL832250	small nuclear ribonucleoprotein polypeptide N	SNRPN	28.0	64.0	1.94	0.004
BC002637	tribbles homolog 2 (Drosophila)	TRIB2	29.1	127.9	1.94	0.014
U55936	synaptosomal-associated protein, 23kDa	SNAP23	118.4	517.0	1.93	0.007
AK027219	---	---	276.1	691.6	1.93	0.013

AI740796	solute carrier family 30 (zinc transporter), member 7	SLC30A7	176.8	442.6	1.93	0.002
NM_004324	BCL2-associated X protein	BAX	197.2	630.0	1.92	0.041
L25629	cathepsin L-like 3	CTSLL3	11.4	27.4	1.92	0.039
AU149503	GTPase activating protein (SH3 domain) binding protein 2	G3BP2	324.9	1006.0	1.91	0.039
AL833286	PDZ and LIM domain 5	PDLIM5	8.6	21.8	1.91	0.019
CA431092	---	---	15.9	37.2	1.91	0.007
NM_017445	H2B histone family, member S	H2BFS	81.8	273.9	1.91	0.028
AW165999	solute carrier family 44, member 1	SLC44A1	41.5	138.9	1.89	0.005
NM_003043	solute carrier family 6 (neurotransmitter transporter, taurine), member 6	SLC6A6	13.9	54.2	1.89	0.014
AF356518	junctional adhesion molecule 3	JAM3	15.2	71.4	1.89	0.013
BG222606	LSM14B, SCD6 homolog B (<i>S. cerevisiae</i>)	LSM14B	7.1	20.5	1.87	0.004
H01893	Rho-related BTB domain containing 3	RHOBTB3	15.0	45.9	1.87	0.041
U16153	inhibitor of DNA binding 4, dominant negative helix-loop-helix protein	ID4	195.5	515.8	1.87	0.026
NM_004612	transforming growth factor, beta receptor I	TGFR1	111.4	641.5	1.86	0.036
AJ000098	eyes absent homolog 1 (<i>Drosophila</i>)	EYA1	12.0	28.6	1.86	0.001
NM_004507	HUS1 checkpoint homolog (<i>S. pombe</i>)	HUS1	8.8	17.7	1.85	0.004
NM_025125	Chromos. 10 open reading frame 57	C10orf57	64.8	134.6	1.85	0.001
AI338705	ubiquitin-conjugating enzyme E2E 3 (UBC4/5 homolog, yeast)	UBE2E3	78.0	190.5	1.85	0.002
BC001281	tumor necrosis factor receptor superfamily, member 10b	TNFRSF10B	26.8	109.4	1.84	0.007
BE500977	sulfatase 1	SULF1	6038.2	14724.0	1.84	0.005
R44149	phosphodiesterase 4D interacting protein (myomegalin)	PDE4DIP	11.9	31.7	1.84	0.008
AI828075	---	---	70.5	216.8	1.83	0.012
NM_005983	S-phase kinase-associat. protein 2 (p45)	SKP2	12.9	64.4	1.83	0.027
AA126728	intercellular adhesion molecule 2	ICAM2	7.6	18.5	1.82	0.040
NM_005966	NGFI-A binding protein 1 (EGR1 binding protein 1)	NAB1	28.9	102.4	1.82	0.047
NM_025239	programmed cell death 1 ligand 2	PDCD1LG2	98.8	253.7	1.81	0.003
AL353759	histone cluster 1, H2bd	HIST1H2BD	50.1	107.8	1.81	0.001
L76416	SMT3 suppressor of mif two 3 homolog 2 (<i>S. cerevisiae</i>)	SUMO2	2816.2	6300.6	1.80	0.036
NM_016613	Chromos. 4 open reading frame 18	C4orf18	71.3	265.8	1.79	0.007

BC002456	voltage-dependent anion channel 3	VDAC3	14.1	41.6	1.79	0.018
NM_004438	EPH receptor A4	EPHA4	6.5	16.3	1.78	0.012
AL514076	tetraspanin 31	TSPAN31	249.7	653.1	1.78	0.016
AF177377	echinoderm microtubule associated protein like 4	EML4	66.2	190.7	1.77	0.009
AK000270	A kinase (PRKA) anchor protein (yotiao) 9	AKAP9	10.8	36.1	1.77	0.020
AI887749	laminin, gamma 1 (formerly LAMB2)	LAMC1	149.2	496.7	1.76	0.030
AW269397	spermatogenesis associated 13	SPATA13	41.1	113.2	1.76	0.031
X06989	amyloid beta (A4) precursor protein (peptidase nexin-II)	APP	1472.9	4405.0	1.75	0.031
U19599	BCL2-associated X protein	BAX	179.9	534.5	1.75	0.032
AV717561	ATPase, H+ transporting, lysosomal 9kDa, V0 subunit e1	ATP6V0E1	73.4	181.2	1.75	0.015
AI962377	PTPRF interacting protein, binding protein 1 (liprin beta 1)	PPFIBP1	114.5	305.5	1.74	0.041
BF110903	BAT2 domain containing 1	BAT2D1	182.2	384.9	1.74	0.004
NM_018153	anthrax toxin receptor 1	ANTXR1	388.8	999.0	1.74	0.035
AV699781	---	---	28.1	91.9	1.74	0.033
NM_005754	GTPase activating protein (SH3 domain) binding protein 1	G3BP1	134.1	411.8	1.73	0.036
AI703321	wingless-type MMTV integration site family, member 5A	WNT5A	747.2	2303.8	1.73	0.017
AY099353	zinc finger protein 655	ZNF655	64.7	209.5	1.73	0.018
AA890010	SEC22 vesicle trafficking protein homolog B (S. cerevisiae)	SEC22B	4061.7	7691.0	1.73	0.001
AL157471	Fraser syndrome 1	FRAS1	108.8	425.5	1.73	0.014
BC006292	transmembrane protein 107	TMEM107	24.2	66.4	1.73	0.014
L18887	calnexin	CANX	672.4	2440.1	1.72	0.006
NM_002716	protein phosphatase 2 (formerly 2A), regulatory subunit A, beta isoform	PPP2R1B	109.9	234.2	1.72	0.007
BF114947	Ras association (RalGDS/AF-6) and pleckstrin homology domains 1	RAPH1	619.7	1457.2	1.72	0.009
AK022804	---	---	22.7	53.4	1.72	0.012
AA743413	eukaryotic transl initiation factor 4B	EIF4B	8.4	21.1	1.72	0.015
AF100751	FK506 binding protein 7	FKBP7	600.7	1438.4	1.72	0.038
N21210	RAB32, member RAS oncogene family	RAB32	28.6	70.7	1.71	0.006
AU147402	caldesmon 1	CALD1	314.0	890.0	1.70	0.026
AC007130	3-hydroxyisobutyrate dehydrogenase	HIBADH	149.2	526.3	1.69	0.013

AW500473	eukaryotic translation initiation factor 4E binding protein 2	EIF4EBP2	9.9	29.5	1.69	0.005
AA765387	hect (homol to the E6-AP (UBE3A) carboxyl terminus) domain and RCC1 (CHC1)-like domain (RLD) 1	HERC1	15.8	34.3	1.69	0.035
NM_002970	spermidine/spermine N1-acetyltransferase 1	SAT1	678.3	1532.5	1.69	0.006
AL550722	transmembrane protein 50A	TMEM50A	3352.8	6754.7	1.69	0.023
AI147738	fucosyltransferase 10 (alpha (1,3) fucosyltransferase)	FUT10	19.9	42.2	1.69	0.002
AP001748	PBX/knotted 1 homeobox 1	PKNOX1	9.1	18.5	1.68	0.034
AK026749	suppressor of defective silencing 3 homolog (S. cerevisiae)	SUDS3	58.1	170.2	1.68	0.017
AL136619	hypothetical protein DKFZp564O0523	DKFZP564O0523	145.2	269.4	1.68	<0.001
AA149655	Chromos. 15 open reading frame 24	C15orf24	58.5	155.9	1.68	0.009
NM_018181	zinc finger protein 532	ZNF532	238.1	629.5	1.67	0.005
D13413	heterogeneous nuclear ribonucleoprotein U (scaffold attachment factor A)	HNRNPU	9.0	25.1	1.67	0.014
AI304862	activity-dependent neuroprotector homeobox	ADNP	41.7	91.7	1.67	0.010
NM_003487	TAF15 RNA polymerase II, TATA box binding protein (TBP)-associated factor, 68kDa	TAF15	168.5	432.1	1.66	0.008
NM_007236	calcium binding protein P22	CHP	22.5	78.2	1.66	0.013
AA724665	---	---	40.0	83.8	1.66	0.009
AI700608	mortality factor 4 like 2	MORF4L2	91.7	237.7	1.65	0.027
NM_014133	sorbin and SH3 domain containing 2	SORBS2	20.3	54.4	1.65	0.025
BE551054	methyltransferase like 9	METTLL9	47.1	134.0	1.64	0.010
AK025037	---	---	99.8	303.3	1.64	0.027
AK002111	karyopherin alpha 6 (importin alpha 7)	KPNA6	26.5	87.0	1.64	0.038
AL121873	ubiquitin-conjugating enzyme E2 variant 1	Kua-UEV	22.9	43.0	1.63	0.008
BC002709	TP53 activated protein 1	TP53AP1	85.6	182.8	1.63	0.009
AI345238	---	---	89.5	266.9	1.63	0.033
AV702101	---	---	63.4	151.7	1.62	0.035
NM_024809	tectonic family member 2	TCTN2	71.5	155.0	1.62	0.004
NM_006792	mortality factor 4	MORF4	3647.0	6658.5	1.62	0.005
BF062335	ASF1 anti-silencing function 1 homolog A (S. cerevisiae)	ASF1A	6.6	17.1	1.62	0.019

NM_017905	transmembrane and coiled-coil domains 3	TMCO3	138.7	298.4	1.62	0.003
BC000282	transmembrane protein 116	TMEM116	17.8	35.7	1.61	0.036
AA100736	SH3 domain protein D19	SH3D19	14.8	55.8	1.61	0.016
AW007319	forkhead box K1	FOXK1	337.9	808.6	1.61	0.038
AF000381	folate receptor 1 (adult)	FOLR1	1698.3	4357.8	1.61	0.037
BE645435	chromos 11 open reading frame 70	C11orf70	48.9	120.2	1.61	0.036
AI953523	seven in absentia homolog 1 (Drosophila)	SIAH1	153.9	350.9	1.61	0.016
BC003092	retinoblastoma binding protein 4	RBBP4	795.0	1622.5	1.60	0.009
AI277316	GLIS family zinc finger 3	GLIS3	56.9	149.0	1.60	0.034
AV652437	AF4/FMR2 family, member 4	AFF4	18.0	101.9	1.60	0.047
BC002382	COX15 homolog, cytochrome c oxidase assembly protein (yeast)	COX15	110.9	193.6	1.60	<0.001
AW163148	myristoylated alanine-rich protein kinase C substrate	MARCKS	431.6	1389.3	1.60	0.011
AI096389	microtubule assoc.serine/threonine kinase family member 4	MAST4	69.0	145.7	1.59	0.003
AV708982	poly (ADP-ribose) glycohydrolase	PARG	21.0	50.4	1.59	0.003
AW418842	polyhomeotic homolog 2 (Drosophila)	PHC2	67.6	166.8	1.59	0.020
NM_018050	MANSC domain containing 1	MANSC1	120.7	346.1	1.58	0.023
BF970340	chromos 1 open reading frame 174	C1orf174	24.2	80.0	1.58	0.019
NM_003999	oncostatin M receptor	OSMR	415.7	1557.0	1.58	0.020
NM_001548	interferon-induced protein with tetratricopeptide repeats 1	IFIT1	20.6	48.8	1.58	0.016
NM_003174	supervillin	SVIL	63.5	234.7	1.58	0.018
BG150485	solute carrier family 6 (neurotransmitter transporter, taurine), member 6	SLC6A6	1629.8	3283.2	1.57	0.025
AU143940	RAR-related orphan receptor A	RORA	34.7	70.6	1.57	0.036
AA778684	solute carrier family 2 (facilitated glucose transporter), member 14	SLC2A14	306.6	673.5	1.57	0.019
AW006345	signal sequence receptor, alpha (translocon-associated protein alpha)	SSR1	722.6	1863.5	1.56	0.015
AK091716	hypothetical protein LOC728190	LOC728190	18.6	50.6	1.56	0.010
BF245482	Cdc42 GTPase-activating protein	CDGAP	57.3	114.7	1.56	0.007
AA813018	tight junction protein 1 (zona occludens 1)	TJP1	138.8	305.6	1.56	0.019
AW241715	ubiquitination factor E4B (UFD2 homolog, yeast)	UBE4B	36.1	115.9	1.56	0.020
NM_004707	ATG12 autophagy related 12 homolog (S. cerevisiae)	ATG12	188.5	589.6	1.56	0.028

N92501	spectrin, beta, non-erythrocytic 1	SPTBN1	71.4	175.0	1.56	0.004
BE646554	TBC1 domain family, member 9 (with GRAM domain)	TBC1D9	19.9	44.8	1.56	0.004
AI890903	potassium channel tetramerisation domain containing 7	KCTD7	82.3	151.7	1.56	0.043
NM_017905	transmembrane and coiled-coil domains 3	TMCO3	87.8	155.2	1.56	0.002
AU147402	caldesmon 1	CALD1	301.5	891.6	1.56	0.029
AU145361	Cas-Br-M (murine) ecotropic retroviral transforming sequence b	CBLB	58.4	120.2	1.55	0.042
NM_018004	transmembrane protein 45A	TMEM45A	2176.0	4118.8	1.55	0.003
AL554245	nuclear receptor subfamily 2, group F, member 2	NR2F2	202.3	653.3	1.55	0.040
AB032963	ATPase, Class I, type 8B, member 2	ATP8B2	627.2	1067.3	1.54	0.004
NM_018934	protocadherin beta 14	PCDHB14	42.7	99.7	1.54	0.016
NM_014456	programmed cell death 4 (neoplastic transformation inhibitor)	PDCD4	107.5	371.3	1.54	0.045
AI888256	ring finger protein 217	RNF217	74.4	149.9	1.54	0.026
AB028839	ubiquitination factor E4B (UFD2 homolog, yeast)	UBE4B	147.8	343.0	1.54	0.036
BF975327	SFT2 domain containing 1	SFT2D1	1334.0	2584.0	1.54	0.007
AW827204	peptidylprolyl isomerase (cyclophilin)-like 4	PPIL4	18.8	56.3	1.54	0.042
BE550486	solute carrier family 2 (facilitated glucose transporter), member 3	SLC2A3	263.7	603.8	1.54	0.039
AF329193	programmed cell death 1 ligand 2	PDCD1LG2	80.8	171.8	1.53	0.038
AF074717	RAD1 homolog (S. pombe)	RAD1	272.3	537.1	1.53	0.027
AW962850	schlafen family member 5	SLFN5	84.0	284.0	1.53	0.020
BE972419	hypothetical gene LOC283846	DKFZp547E087	71.7	296.4	1.53	0.014
AI016620	signal sequence receptor, alpha (translocon-associated protein alpha)	SSR1	1387.0	2689.2	1.53	0.012
J03263	lysosomal-assoc. membrane protein 1	LAMP1	210.5	917.5	1.53	0.040
BE910600	MyoD family inhibitor domain containing	MDFIC	151.3	367.3	1.53	0.011
AB007900	signal-induced proliferation-associated 1 like 1	SIPA1L1	336.1	596.5	1.53	0.018
X15132	superoxide dismutase 2, mitochondrial	SOD2	177.1	410.9	1.52	0.047
NM_017712	pyroglutamyl-peptidase I	PGPEP1	15.2	45.6	1.52	0.045
BE967311	mutated in colorectal cancers	MCC	93.2	314.9	1.52	0.020
BC040053	methionine sulfoxide reductase B3	MSRB3	105.9	272.2	1.51	0.007

NM_025076	UDP-glucuronate decarboxylase 1	UXS1	351.2	661.3	1.51	0.002
AA716107	sushi, von Willebrand factor type A, EGF & pentraxin domain containing 1	SVEP1	93.1	337.7	1.51	0.015
BC005369	egl nine homolog 1 (C. elegans)	EGLN1	256.8	477.1	1.51	0.002
A1557425	ribosomal protein L23a	RPL23A	465.9	927.9	1.51	0.010
NM_001904	catenin (cadherin-associated protein), beta 1, 88kDa	CTNNB1	2200.5	3806.3	1.51	0.003
AF362887	---	---	32.2	70.1	1.51	0.040
NM_003825	synaptosomal-associated protein, 23kDa	SNAP23	186.6	701.1	1.51	0.017
AL041728	slingshot homolog 1 (Drosophila)	SSH1	529.4	993.8	1.51	0.011
NM_014423	AF4/FMR2 family, member 4	AFF4	39.9	71.3	1.50	0.003
BC005343	dynein, axonemal, light chain 1	DNAL1	22.2	60.7	1.50	0.012
U28936	tyrosine 3-monooxygenase trypto-phan 5-monooxygenase activation protein, epsilon polypeptide	YWHAE	178.7	683.2	1.50	0.024
AF080569	DnaJ (Hsp40) homolog, subfamily B, member 6	DNAJB6	773.0	1902.5	1.50	0.026
BG252842	Chromos. 6 open reading frame 62	C6orf62	251.5	755.8	1.50	0.023

1 average expression level in young age group; 2 average expression level in old age group; 3 differential expression;
4 p-value was calculated using Student's T-test (two-tailed, two-sample, unequal variance)

Supplementary Table 4: gene-specific primer pairs applied in quantitative reverse transcription PCR

Gene Symbol	Gene Name	forward / reverse primer (5'-3')	amplicon [bp]	TM [°C]	Ensembl Transcript ID
ALPL	Alkaline phosphatase, tissue-nonspecific isozyme precursor	CTTCAAACCCGAGATACAAGC TCAGCTCGTACTGCATGTC	125	60	ENST00000344573 / ENST00000374832 / ENST00000374840
EEF1A1	Elongation factor 1-alpha 1 (EF-1-alpha-1)	CAAGTGCTAACATGCCTTGGT GAACAGTACCAATACCACCAATTT	177	60	ENST0000309268 / ENST0000316292 / ENST0000331523
FABP4	Fatty acid-binding protein, adipocyte	GCTTTGCCACCAGGAAAGT GGACACCCCATCTAAGGTT	195	60	ENST00000256104
IBSP	Bone sialoprotein-2 precursor	CCGAAGAAAATGGAGATGACAG CCATAGCCCAGTGTGTAGCA	145	60	ENST00000226284
ITGA3	Integrin alpha-3 precursor (CD49c antigen)	CACCTTCATCGAGGATTACAGA AGTCAATGTCCACAGAGAACCA	131	60	ENST00000007722 / ENST00000320031
LEPR	Leptin receptor precursor (CD295 antigen)	CCTCTTCATCTTATTGCTTGG GCTCAAACGTTTCTGGCTTCT	154	60	ENST00000349533
LPL	Lipoprotein lipase precursor	GTGGCCGAGAGTGAGAACAT TCCACCAGTCTGACCAGCTA	157	60	ENST00000311322
NANOG	Homeobox transcription factor Nanog	CAGATGCAAGAACTCTCCAACA TGAGGCCTTCTGCGTCACA	141	60	ENST00000229307 / ENST00000396598
PMF1 / BGLAP	Polyamine-modulated factor 1 (osteocalcin)	ATCAAAGAGGAGGGGAACCTA AGGAAGTAGGGTGCCATAACA	143	60	ENST00000368277 / ENST00000368280
PPARG	Peroxisome proliferator-activated receptor gamma	TACATAAAGTCCTTCCCGCTGA GGGGTGATGTGTTGAACCTG	143	60	ENST00000309576 / ENST00000287820 / ENST00000396998 / ENST00000397003 / ENST00000397006 / ENST00000397010 / ENST00000397012 / ENST00000397015 / ENST00000397023 / ENST00000397026
SPARC	SPARC precursor (Secreted protein acidic and rich in cysteine) (osteonectin)	TCCCTGTACTGTCAGGTC TCCAGGTCACAGGTCTCG	142	60	ENST00000231061
SPP1	Osteopontin precursor (bone sialoprotein-1, secreted phosphoprotein 1)	CACCTGTGCCATACCAGTTAAA AGCATTCTGTGGGGCTAGG	142	60	ENST00000395080
UTF1	Undifferentiated embryonic cell transcription factor 1	CAGCGAACCCAGACGCCAC GTCCTCGGGGATGCAGGT	169	60	ENST00000304477
VCAM1	Vascular cell adhesion molecule 1 (CD106 antigen)	TGGGAAAAACAGAAAAGAGGTG CCAGGAGAAAAGATGGGGATT	151	60	ENST00000294728 / ENST00000370119 / ENST00000347652 / ENST00000370115
ZFP42	Zinc finger protein 42 (REX-1)	CTTGAGCCCAGGAGTTTGAG GGGCTATGACATGAACCATGA	132	60	ENST00000326866

